Scientific Research Publishing

Open Journal of Geology, 2021, 11, 105-141
https://www.scirp.org/journal/ojg
ISSN Online: 2161-7589
ISSN Print: 2161-7570

Petro-Structural Study of the Paleoproterozoic Formations of the Faboula Gold Deposit (Bougouni-Kékoro Basin, Leo-Man Shield)

Ousmane Wane[1*], Amadou Baby Ouologuem[1], Ismaïla N'diaye[2], Ousmane Dao[2], Mamadou Yossi[3]

[1]Laboratoire de Minéralogie et de Pétrologie, Faculté des Sciences et Techniques, Université des Sciences, des Techniques et des Technologies de Bamako, BP E 3206, Colline de Badalabougou, Bamako, Mali
[2]Faculté des Sciences et Techniques, Université des Sciences, des Techniques et des Technologies de Bamako, BP E 3206, Colline de Badalabougou, Bamako, Mali
[3]Sagax Afrique S.A Geophysical Surveys and Consulting, Ouagadougou, Burkina Faso
Email: *ousmane.wane@gmail.com

How to cite this paper: Wane, O., Ouologuem, A.B., N'diaye, I., Dao, O. and Yossi, M. (2021) Petro-Structural Study of the Paleoproterozoic Formations of the Faboula Gold Deposit (Bougouni-Kékoro Basin, Leo-Man Shield). *Open Journal of Geology*, **11**, 105-141.
https://doi.org/10.4236/ojg.2021.114007

Received: March 10, 2021
Accepted: April 23, 2021
Published: April 26, 2021

Abstract

Recent petro-structural investigations on the Faboula gold deposit located in the Bougouni-Kékoro basin, in southern Mali, north-west of the Leo-Man Shield, have provided new data on the nature and spatial organization of the lithostratigraphic units as well as their deformation style. The deposit is covered by a thick lateritic layer and is hosted by a metavolcano-sedimentary sequence of Paleoproterozoic age intersected by intrusive bodies and filled fractures of various shapes and types. The lithostratigraphic units consist of metagreywackes, metasiltstones, meta-argillites, slates and schists. Metagreywackes and metasiltstones are generally feldspathic, both may contain biotite and locally amphibole, just as slates may contain andalusite which is locally stretched. Plutonic units most often occur as stocks or as dikes on the drill core, up to 1 m. The metavolcano-sedimentary rocks are schistose and deformed under greenschist facies conditions, and locally they reach the epidote-amphibolite facies. The structural study revealed that the deposit is affected by several stages of deformation evolving from a ductile type to a brittle type via a ductile-brittle type. The dominant ductile and brittle-ductile deformations show a combination of isoclinal folding and strike-slip faults. Both the isoclinal folding and the strike-slip faults whose sigmoidal en-echelon tension gashes indicate a dextral movement in the NNE-SSW direction are the result of the same ENE-WSW regional shortening. Consequently, they highlight a transpressive deformation. This deformation noted here D_{2Fb}, could be equivalent to the regional D_2 or D_3 deformations identified at the scale of the Leo-Man Shield if we refer to the style of deformation. There is an abundance

of quartz veins networks. Their relation within the structural features indicates that the mineralization is structurally controlled during a hydrothermal event linked certainly to the circulations of fluids during the transpressive event D_{2Fb}.

Keywords

Faboula, Gold, Deposit, Metavolcano-Sedimentary Rocks, Deformation, Paleoproterozoic, Transpression, Drill Cores, Southern Mali, Leo-Man Shield

1. Introduction

West Africa Craton (WAC) has become the target of gold exploration and exploitation by the major global mining companies because of its world-class gold deposit and the increase of the price of the precious metal.

This interest triggered the development of a lot of scientific research and industrial projects among national geological surveys, mining companies and universities for a better understanding of the geological evolution of the WAC. The interest also allowed the discovery of numerous gold deposits and the detection of areas of high-potential gold mineralization. Gold deposits in the WAC are principally hosted in the Paleoproterozoic formations, also known as Birimian formations, which developed between ca. 2312 - 2060 Ma according to the integration of the previous works of many authors [1]-[16]. Many gold deposits have also been found in land of similar age in Australia, Canada, China, etc. Half of the world's gold reserves are in the Precambrian formations [17].

Mali is renowned for its wealth in gold, at least since the Middle Age [18]. In 1433 the pilgrimage to Mecca of the famous emperor Kankou Moussa helped to amplify this reality. However, the country only became an industrial exporter of this ore very recently, in the mid-1980s with the exploitation of the Kalana gold deposit. Since then, gold mining has experienced a boom, favoured by the installation of many mining companies. Nowadays, thirteen modern mines have emerged in Mali, seven in the west of the country and six in its southern counterpart including the Faboula gold deposit (FGD).

The economic importance taken by gold in recent years has pushed mining companies to leap into new research opportunities on gold and beyond all the mineral resources present in the Birimian of Mali. Projects combining both the establishment of geological maps and the prospecting of natural substances have been carried out. They led the country to rank Third African Gold Producer after South Africa and Ghana in less than a decade. The gold reserves are estimated at over 800 tons [19] and its production was 2.14 Moz (60.7 t) in 2018. It leads export product ahead of the cotton and the cattle breeding. The contribution of the mining sector in Mali's export is around 63.3% and its apport in the GDP is roughly 6.6%. In 2017 Gold production gave Mali a total of 405.30 million USD [19]. Paradoxically, the geology of the Birimian of Mali is still un-

known particularly in the south of the country where the study area, the FGD, is located.

FGD belongs to the western part of the Bougouni-Kékoro basin which is crossed by an abundant network of large rivers whose alluvium abundantly covers the Birimian rocks. In addition, the particularly plentiful and continuous lateritic cover masks considerably the outcrops. The coupling of the intense lateralization and the scarcity of the outcrops constitutes a challenge for geologists.

The investigation of the Birimian of Mali requires the integration of some information on satellite data, geophysics, field and laboratory works, regolith mapping, inventory of artisanal mining sites, geochemical survey of soils and subsoils, drilling data specially diamond drilling data, etc. The use of each piece of information provided by all these methods of studies solves the problem of lack of information on the surface. However, the combination of field observations, laboratory analyses, and drill core dataset constitutes a relevant approach for the identification of the lithologies and the structures of a region. They solve a large part of the problem induced by the spatial and temporal distribution of the hidden geological information. This last scheme is adopted by the present study. The field work provides solid data in terms of lithologies, tectonic and relative geochronology. The diamond drill cores give access to underground information. It yields knowledge on the lithologies and structures of the formations in depth and their associated mineralization and allows to identify the extension of this one.

This article brings a new set of field, laboratory, and drill cores data. It aims to identify the petrographic characteristics of the Faboula gold deposit, to characterize the local stratigraphic column as well as the different tectonic phases that affect the area and to replace the local tectonic evolution within the regional structural framework of the Leo-Man Shield.

2. Geological Setting

2.1. Regional Geological Setting of the Paleoproterozoic of Southern Mali

The FGD is located on the northwestern margin of the Leo-Man Shield (**Figure 1**), southern part of the West African craton (WAC) which was identified in 1964 by [20]. This craton is bounded, by the Pan-African folded and metamorphosed mobiles belts: to the west by the Rockelides and the Mauritanides belts and to the east by the Pharusian and the Dahomeyan belts. The WAC has been stable since 1700 Ma [2] [21] [22]. This assertion was recently confirmed by the work of [23], who identified the presence of a late Paleoproterozoic sequences (~1.75 Ga) in the Anti-Atlas of Morocco, in the far north of the WAC.

The WAC is exposed in two major shields (Reguibat and Leo-Man Shields) and in three inliers (Kédougou-Kéniéba, Kayes and Anti-Atlas inliers). The two shields are separated by the Upper Proterozoic to Late Paleozoic sediments of the Taoudeni basin. The Reguibat Shield in its northern parts and the Leo-Man

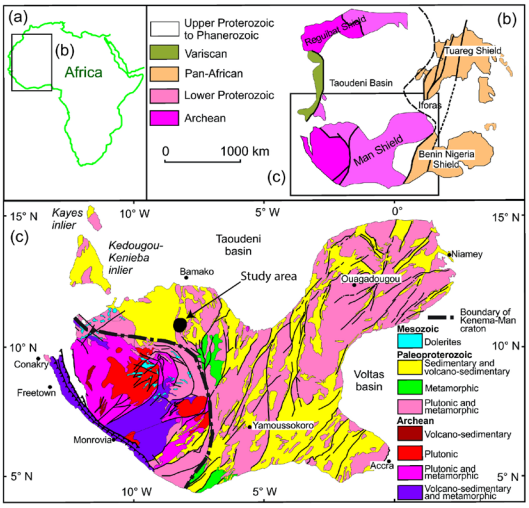

Figure 1. (a) Simplified map of Africa. (b) Simplified geological maps of the West African Craton after [26]. (c) Simplified geological map of the Leo-Man Shield, after [66], with localization of study area (black circle).

Shield in its southeastern parts are covered respectively by the Paleozoic basin of Tindouf and the Neoproterozoic basin of Volta [22] [24] [25].

The Leo-Man Shield covers Senegal, Mali, Burkina Faso, Niger, Ivory Coast, Ghana, Guinea, Liberia, Sierra Leone and the Extreme north of Togo. It comprises two distinct domains separated by the Sassandra Fault Zone: a western Archean domain called the Kénéma-Man domain and an eastern Paleoproterozoic (Birimian) domain known also as the Baoulé-Mossi domain. The latter hosts the FGD in its northwestern part (**Figure 1**).

The Kénéma-Man domain forms the basement of nearly all Sierra Leone and Liberia, southeastern Guinea and a small part of the western of Ivory Coast. It is constituted by the association of greenstone belts and granitoids [24] [26] [27] [28] [29]. It is made up of migmatites, charnockites, orthogneiss, paragneiss, banded iron formations (BIFs) and metamorphosed formations represented by amphibolites and granulites [22] [27]-[34]. According to these authors the Archean rocks underwent meso to catazonal metamorphism and were migmatized more or less locally.

The Archean domain was modelled by two tectono-magmatic events: the Leonian (~3244 - 2900 Ma) and the Liberian (~2900 - 2700 Ma) [24] [27] [29] [35]. An earliest evidence for continental accretion of Archean age (3542 ± 13 Ma) in the Leo-Man Shield has been recognized in Guinea on the basis of zircon dating [29]. This result has been confirmed by [34], who obtained a Nd model age of 3456 Ma, on the tonalitic gneiss of Balma, of the SASCA area located in south-western Ivory Coast.

The Baoulé-Mossi domain crops out in Guinea, Senegal, Mali, Burkina Faso, Niger, Ivory Coast, Ghana and in the extreme of northern Togo. It is formed by the association of narrow greenstone belts and large volcano-sedimentary basins both have been intruded by several generations of granitoids. The volcanic and

the sedimentary rocks of the Leo-Man Shield are termed Birimian [36] [37] and considered as supracrustal rocks. They were emplaced between ca. 2255 - 2060 Ma according to the integration of the previous works of many authors [2] [3] [5] [6] [8] [9] [10] [11] [15] [16] [38].

The greenstone belts are slimmed and oriented curvilinear entities made up of various volcanic rocks and subordinate detrital rocks. They were principally deposited between ca. 2250 and 2180 Ma, however their formation continued until about ca. 2100 Ma [11]. They are represented by lavas, volcanoclastic and siliciclastic rocks. The lavas have a variable chemical composition ranging from basalt to rhyolite with a tholeiitic or calc-alkaline affinity [1] [2] [3] [4] [39]-[44]. The volcanoclastic and siliciclastic rocks are represented by greywackes, shales, and sandstones (flysch-type) and locally by molassic deposit (conglomerates, feldspathic sandstones, and minor argillites). According to [16] they display a NE-SW to N-S orientation in the eastern and central Baoulé-Mossi domain, while in its west part they are oriented N-S to NW-SE. Several authors noted that their emplacement indicates diachronously volcanic activities from east to the west with the oldest volcanogenic rocks preserved in the eastern part of the Baoulé-Mossi domain and the youngest in its western part [6] [16] [44].

Volcano-sedimentary basins are the deposition environments of flysches in which intercalations of subordinate lavas and volcaniclastic rocks are found. They are made up of greywackes, siltstones, argillites, schists, lavas, volcaniclastic rocks and occasionally manganiferous, carbonate and/or siliceous chemical rocks. Carbonate rocks are found mainly in the Siguiri basin and Kédougou-Kéniéba inlier [38] [45] [46] [47] [48] [49]. As well as the volcanic activities, the sedimentary sequences show similar migration from east to west. Maximum depositional ages are in the range of 2160 to 2130 Ma in the east and 2110 - 2065 Ma in the west [16].

The granitoids are abundant throughout the Baoulé-Mossi Domain. They are closely associated with the supracrustal rocks. They display various mineralogical and geochemical compositions as well as geochronological characteristics and diverse settings. They are represented principally by tonalite, trondhjemite, granodiorite (TTG), gneisses, diorites and granites. They were emplaced between ca. 2312 and 1980 Ma according to several works [1] [3] [4] [6] [7] [10]-[15] [43] [50] [51] [52] [53]. The peak of magmatic activity is around 2100 Ma [3] [4].

All the Paleoproterozoic formations have been affected by the polycyclic deformation and metamorphism of Diachronous Eburnean Orogeny between ca. 2270 and 1960 Ma [3] [7] [10] [11] [15] [16] [44] [54] [55] [56] and references therein. This orogeny defined by [57] has a polyphase character according to many authors [6] [26] [54] [58] [59]. It has undergone major style of tectonics: a transpressive deformation responsible of the crustal thickening of the units and a transcurrent deformation responsible of the movements along the shear zones. The latter postdated the former.

Different models have been suggested for explaining the terms of the assembling of the accreted segments, in the case of the thickening of the Birimian

crust, and it's joining to the Archean block. Some authors proposed an archaic type of model highlighted by gravity driven tectonic processes [42] [59] [60]. Others suggested a modern type integrated in the processes of plate tectonic with folding, oblique collage of terranes, functioning of major thrust [7] [15] [54] [55] [58] [61] [62]. The record of basic to acidic volcanism, flysch-type sedimentation, and subsequent compressional deformation, uplift and molasse formation preserved in the Birimian Group resembles a complete Phanerozoic orogenic cycle [63].

In the Malian part of the Baoulé-Mossi domain, the geology is quite poorly constrained due to the limited outcrops and the lack of drilling in certain areas. According to [64], there are three main basins and two principal volcanic greenstone belts (**Figure 2**). The basins are represented from East to West by the Bagoé basin, the Bougouni-Kékoro basin and the Siguiri basin and the greenstone belts are the Syama Belt and the Yanfolila Belt (**Figure 2**). Two main shear zones, Syama Shear Zone and Siekorolé Shear Zone, both oriented N-S to NNE-SSW, crosscut the greenstone belts and one, the Banifing shear Zone, separates the Bagoé Basin from the Bougouni-Kékoro Basin.

A synthetic chronology of the evolution of the Birimian of southern Mali has not yet been carried out. However, on the basis of the dating rocks, the intrusions of the Massigui region were emplaced between the ca. 2115 - 2074 Ma period [3] [15] [65], while the volcano-sedimentary sequences record a longer period: 2125 to 2090 Ma [3] [15]. But if we take into account the first evidence of Birimian volcanic manifestation, identified at the border of Guinea and Mali by

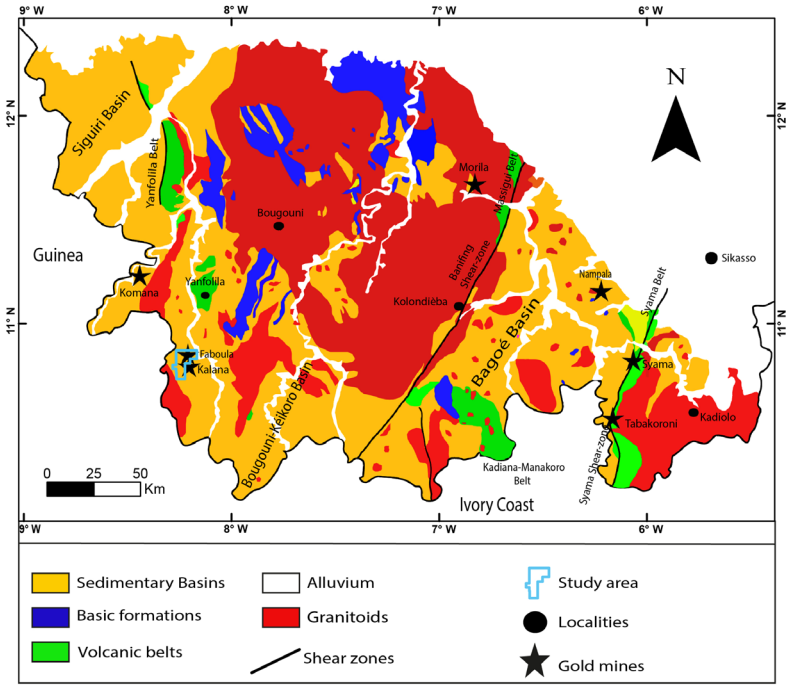

Figure 2. Simplified geological map of the Paleoproterozoic of southern Mali, after [64] with localization of the study area (blue frame).

[8] on a sample from rhyodacite of the Niani volcanic suite, we can extend it to ca. 2212 - 2090 Ma. No Archean ages have been recorded in the sediments from the Massigui region [15] and references therein. However, a small group of detrital zircons from the Bani River in the western part of the Yanfolila greenstone belt gave U-Pb ages between 3.6 and 2.7 Ga [13]. The authors suggested that this group is the result of distal transport from the Archean Kénéma-Man domain.

2.2. Local Geological Setting of the Faboula Gold Deposit

The FGD is located in southern Mali, at the limit of the western edge of the Bougouni-Kékoro basin, not far from the Yanfolila greenstone belt and near the Kalana gold deposit (**Figure 2** and **Figure 3**).

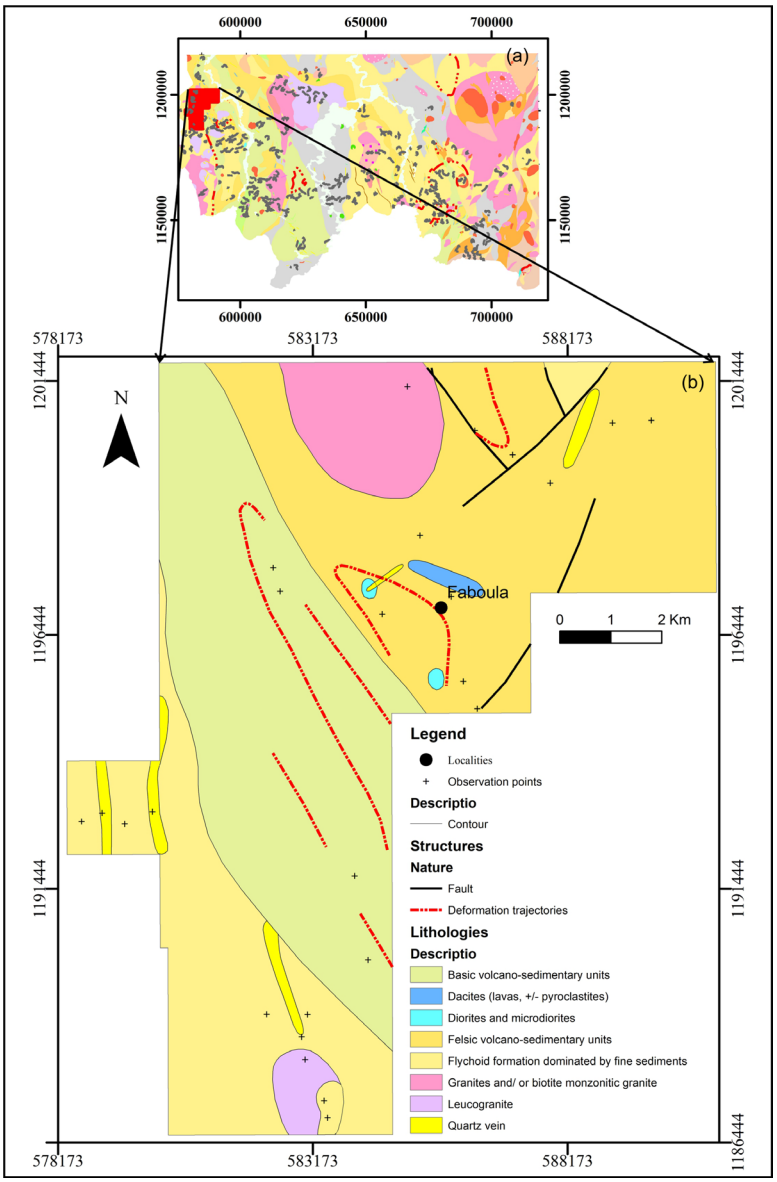

Figure 3. (a) Geological map of the Tienko Sheet (southern Mali) after [67]. (b) Extract of the geological map of Faboula Gold deposit with minor modification.

The Bougouni-Kékoro basin is made up of discontinuous lands of metavolcano-sedimentary rocks intruded by various plutonic rocks belonging in large part to a batholithic complex, which is a continuation of the Massigui batholith. The basin hosts a spectacular swarm of spodumene bearing pegmatites.

The lithostratigraphic units of the basin contain flysch type unit, basic and acid volcano-sedimentary rocks [67] [68] [69]. They are principally represented by metagreywackes and metavolcano-sedimentary formations, and the former is topped by the latter. The metagreywackes formations are volcano-sedimentary deposits most often of intermediate composition; they are formed by conglomerates, arkoses interbedded with pyroclastic and lavas flow, most often andesitic in composition. The metavolcano-sedimentary formations include dominant flyschoid formation constituted mainly by fine-grained sediments, siltstones and argillites, which are intercalated with feldspathic sandstone. Volcano-sedimentary deposits, basic at the base and acidic upwards, are intercalated in the flysch-unit [67].

The volcano-sedimentary rocks are deformed and metamorphosed generally into greenschist facies. They have been dated from 2212 ± 6 Ma to around 2100 Ma; the oldest age, obtained by Pb-Pb evaporation on zircon, has been found on the Niani volcanic suite which has been identified and characterized in Guinea by [8], and recognized in Mali by [68]. It is composed of porphyry lavas and pyroclastic rocks (bedded tuffs, pyroclastic breccias) of andesitic to rhyodacitic composition. Its occurrence is the earliest volcanic event identified to date in Guinea and Mali.

The geology of the FGD is still unclear, the facies are hided under a very dense lateritic cover, about 40 to 90 m which prevents any surface geological work; access to the unaltered rocks is only possible by boreholes. The map of the mine, according to [67] [68], shows the predominance of the flyschoid deposits of the metavolcano-sedimentary formations (**Figure 3**). As stated by [70], the FGD is hosted by an acid volcano-sedimentary series metamorphosed to greenschist facies. The metasedimentary series correspond to the fine and coarse-grained terrigenous sediments (siltstones, mudstones, arenites, quartz-arenites, arkoses and microconglomerates). They are affected by schistosity, generally subparallel to the stratification, oriented N150 to N180 with a steep dip varying from 50˚ to 90˚ towards W or SW. The metasedimentary series is cut by intrusive and vein rocks, inducing contact metamorphism with formation of granofels [70].

3. Materials and Methods

The petrographic and structural characterizations of the FGD presented many difficulties due in part to the absence of outcrops or their weakness. The deposit is affected by very deep lateralization which only revealed rare exposures of altered terrain. In order to solve these field constraints, the petrographic study was realized mainly but not exclusively on the drill cores where the sampling was done. The structural study was conducted in the two open-pits called Main Zone and Zone 5, and on the drill cores.

The petrographic study consists of macroscopic and microscopic descriptions. Thirteen samples representative of the lithologies of the deposit were selected: six samples of metavolcano-sedimentary rocks, four samples of plutonic rocks and three samples of quartz veins. These rocks were sampled from six drill cores previously chosen because of the freshness of their samples. Optical microscopy was achieved, on polished thin sections made at the University of Lisbon, in the Mineralogy and Petrology Laboratory of the Faculty of Sciences and Techniques (FST) of University of Sciences, Techniques and Technologies of Bamako (USTTB), using Olympus BX-53 P equipped with connected Olympus HD camera (DP 73).

The establishment of the stratigraphic column proposed here was carried out on a representative borehole (KDDD16-470) of the core drillings.

The boreholes selected for the structural study are the oriented holes KDDD16-572 and KDDD16-573. The structural measurements on the oriented drill cores were carried out using a device called "Rocket". This device is equipped with a compass and clinometer. Its proper use consists, first of all, in orienting it according to the direction and the dip of the borehole. The drill core is then placed in the axis of the "Rocket" so that the orientation line on the drill core coincides with the axis of the device. Knowledge of the depth of the structures measured on the drill core in a borehole is essential during a microstructural study because it can confirm or invalidate the surface data.

The results on the petrographic analysis are presented in Figures 4-7, the stratigraphic column is given by Figure 8, and the structural analysis by Figures 9-12.

4. Results

4.1. Lithologies

The lithologies of the FGD consist of dominant quartzofeldspathic metavolcano-sedimentary rocks intersected by plutonic rocks of intermediate composition. The petrographic study has been carried out on thirteen selected drill cores samples representative of the major rocks of the deposit.

4.1.1. Metavolcano-Sedimentary Rocks

The metavolcano-sedimentary rocks of the FGD represent a very deformed sequence of flysch type. In general, they strike NNW-SSE and dip steeply (50˚ to 90˚) towards SW. The main facies are metagreywackes, metasiltstones, meta-argillites, slates and schists. Samples were taken from the facies that could be studied in the polarized light microscope.

1) Amphibole bearing volcanoclastic metagreywacke: Sample 468 E4-a

On a macroscopic scale, the rock is dark grey, and varies from medium-grained (clasts of ≤0.5 mm) to coarse-grained (clasts up to 2 mm) with sub-rounded clasts of feldspar and quartz (Figure 4(a)). It contains carbonate as well as disseminated sulphides.

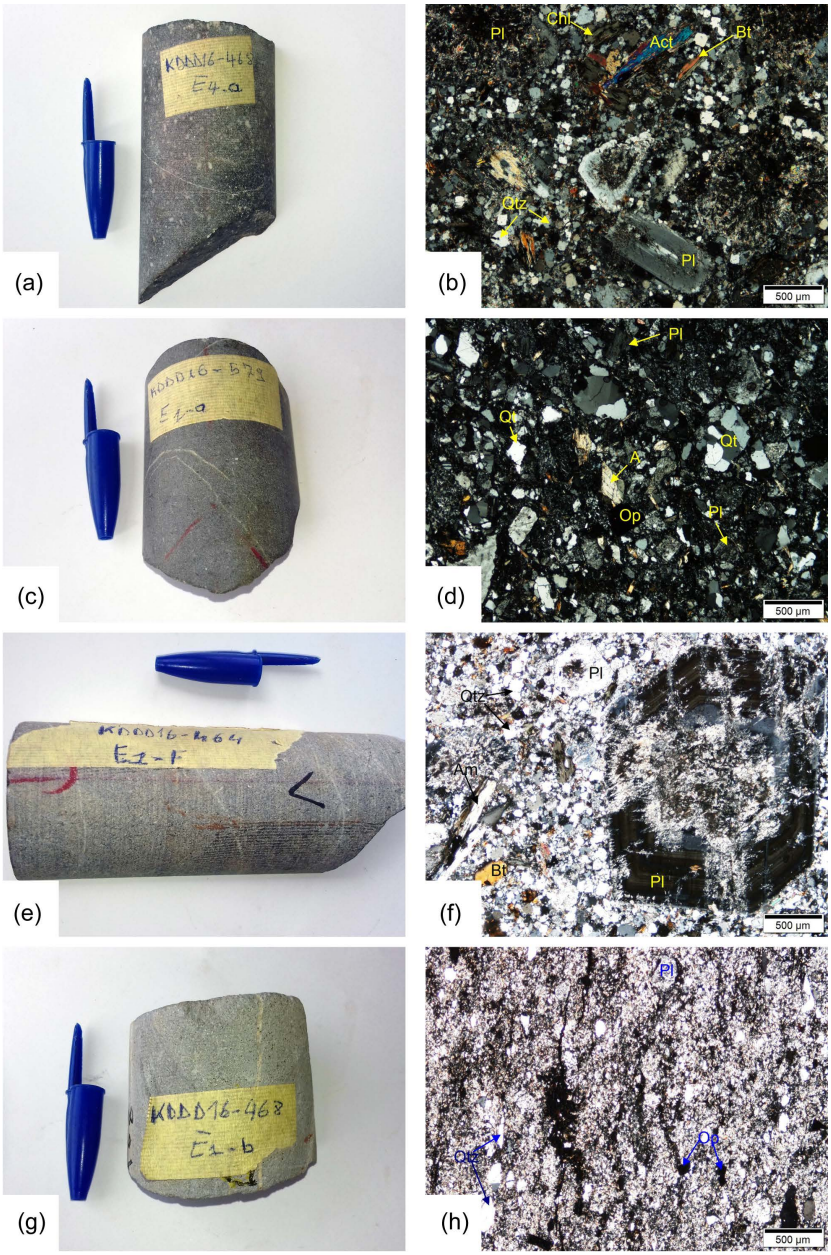

Figure 4. Macroscopic and microscopic pictures of some samples of metavolcano-sedimentary rocks. (a) and (b) Amphibole bearing volcanoclastic metagreywacke. (c) and (d) Amphibole-sulphide bearing volcanoclastic metagreywacke. (e) and (f) Amphibole-biotite bearing volcanoclastic metagreywacke. (g) and (h) Sulphide bearing quartzo-feldspathic schist.

Under the microscope, the rock shows a granoblastic texture (**Figure 4(b)**). The clastic fraction of the rock is constituted of plagioclases, quartz and lithic fragments in a poorly sorted recrystallized matrix.

The plagioclases are the most abundant coarse clastic fraction of the rock, they are euhedral to subhedral, cloudy or brownish-coloured and altered. They show varying size, from micrometric to millimetric (0.5 to 2.1 mm) and can be identified by polysynthetic twins or zoning. Their alteration gives a mixture of sericite

and epidotes. The quartz is micrometric, angular to sub-rounded; its size is up to 250 μm. The lithic fragments are mainly constituted by plagioclases fragments.

The matrix of the rock is made up of an inequigranular, fine-grained assemblage of minerals, composed predominantly of quartz, with a lower proportion of plagioclases, biotite, actinolite, chlorite, epidote, calcite and opaque minerals. Actinolite is randomly oriented; it is pleochroic in shades of green and developed on the clastic fraction of the rock. The mineral occurs dominantly as aggregates of elongated prismatic crystals, occasionally as hexagonal prisms. Its size varies from micrometric to millimetric (up to 2.3 mm), some crystals show twinning. Biotite is brown, micrometric to millimetric (0.07 to 1.3 m) but generally micrometric. It is sometimes pseudomorphosed by chlorite which can develop from biotite or amphibole.

The other minerals present but in low proportion are: epidote, sericite, calcite, apatite, rutile and opaque minerals.

2) Amphibole-sulphide bearing metagreywackes: Sample 579 E1-a

The rock color is grey and fine to medium-grained (**Figure 4(c)**). It contains sulphides and carbonates evidenced by their reaction with HCl.

Under the microscope, the rock shows granoblastic texture (**Figure 4(d)**), with random orientation of the clastic grains.

The clastic fraction of the rock is fine to medium-grained. It is composed of plagioclases, quartz, and lithic fragments embedded in a poorly sorted and recrystallized matrix. The matrix, very fine-grained consists of quartz, feldspars, calcite, epidote, chlorite and sulphides.

Feldspar is micrometric plagioclases, up to 300 μm. They are cloudy or brownish-coloured, much altered and often recrystallized into fine grains. Quartz is subrounded to subangular, it is micrometric in size, up to 600 μm and contains fluid inclusions. It appears as single crystal or polycrystalline, and both show undulose extinction as a result of strain. The boundaries between polycrystalline quartz are sometimes sutured. The lithic fragments are mainly composed of fragments of shale or slate. The rock contains also a fragment constituted of plagioclases laths set in an altered fine-grained groundmass; it is probably a volcanic rock fragment.

The matrix consists of fine-grained quartz, plagioclases, amphibole, chlorite, sulphides, and calcite. Some grains of plagioclases show polysynthetic twins. Amphibole is pleochroic in the shades of green; it is a micrometric hornblende, up to 450 μm, which developed on the quartz-feldspar grains. It occurs as euhedral to subhedral, sometimes it is replaced by chlorite. Calcite is micrometric and presents variable forms: some individuals have anhedral to subhedral shapes. Sulphides are micrometric up to 360 μm, they occur often as well shaped with square form, they are dominantly pyrite.

3) Amphibole—biotite bearing volcanoclastic metagreywacke: Sample 464 E1-f

The rock is light grey in color, medium to coarse-grained and is crossed by carbonate veins (**Figure 4(e)**).

Under the microscope, it shows an inequigranular granoblastic texture (Figure 4(f)); grains are randomly oriented. The clastic fraction of the rock consists mainly of plagioclases, and secondarily of quartz, all dispersed in a poorly sorted recrystallized matrix. Quartz and plagioclases show locally angular fragments, some with remnants of crystal faces.

Plagioclases are coarse-grained and abundant in the clastic fraction. They are micrometric to millimetric and they reach 2.5 mm. They show different shape, from euhedral to subhedral type, prismatic to angular. Most of the euhedral ones are strongly zoned. Quartz, of micrometric size up to 250 μm is abundant in the fine-grained matrix. It is angular to subrounded with locally some straight borders and discrete gulf corrosion. Some grains present undulose extinction. The lithic fragments are composed of an assemblage of dominant plagioclases and minor quartz.

The matrix is fine-grained and poorly sorted. It is composed of quartz, plagioclases, amphibole, biotite chlorite, calcite epidote and opaques minerals. Amphibole is micrometric to millimetric, up to 1.5 mm, it occurs either as free or in an aggregate. It is replaced mainly by chlorite and appears locally retromorphic. Biotite is brown, micrometric up to 880 μm, sub-automorphic and strongly pleochroic. It contains occasionally rutile. Biotite is quite often replaced by chlorite, which replaces amphibole as well.

Secondary minerals such as calcite, epidote and opaques minerals are also present in small amounts.

4) Sulphide bearing quartzofeldspathic schist: Sample 468 E1-b

The rock is grey in colour, medium-grained, and consists mainly of quartz with a dissemination of sulphides in the matrix (Figure 4(g)). The rock is cut by veinlets (~1 - 2 mm) composed of the quartz-carbonate-sulphide association.

Under the microscopic, the rock shows a foliated texture (Figure 4(h)); marked by orientation of elongate quartz and rare plagioclases.

The clastic fraction of the rock consists of dominant quartz and very minor altered plagioclases. The quartz is stretched and micrometric, in general up to 550 μm. It shows locally polycrystalline form composed of granoblastic grains with triple junction at 120˚. The rare grains of plagioclases, up to 300 μm, are unrecognizable, most of them are strongly altered and give a mixture of micrometric grains of sericite and epidote.

The matrix consists of very fine-grained quartz, feldspar, sericite, carbonate, epidote and opaque sulphide-type minerals.

5) Andalusite hornfels: Sample 464 E2-b

The rock is dark-coloured and made up of very fine unrecognizable grains with the naked eyes or with a magnifying glass (Figure 5(a)).

Under the microscope, the rock presents a granoblastic texture (Figure 5(b)). It mainly contains porphyroblasts of andalusite and secondary grains of quartz and plagioclases, both are embedded in a very fine clay matrix that appears dark and indistinct.

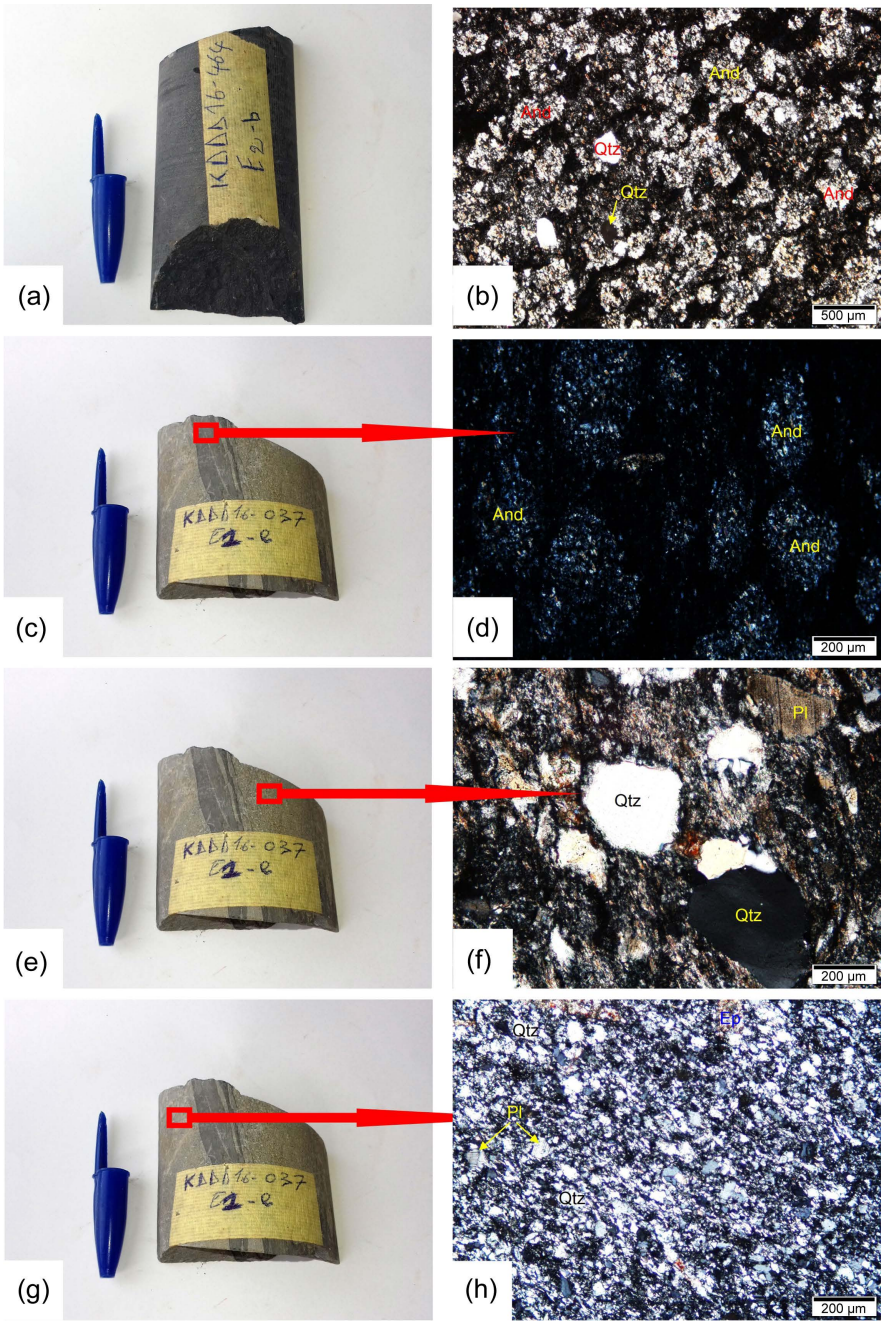

Figure 5. Macroscopic and microscopic pictures of some samples of metavolcano-sedimentary rocks. (a) and (b) Andalusite hornfels. (c) and (d) Andalusite slate. (e) and (f) Feldspathic metagreywacke. (g) and (h) Feldspathic metasiltstone.

The porphyroblasts of andalusite are altered, many of them occur as euhedral to anhedral and appear in rhombic-shaped to weakly elongated. They are micrometric, (up to 500 µm), and colourless in plane-polarized light; in cross-polarized light, they show a mixture of sericite, chlorite and opaque minerals. Andalusite shows locally numerous dark inclusions arranged in the centre, and propagate towards the diagonals, drawing a typical cruciform pattern of graphite rich inclusions. This type of andalusite is commonly called chiastolite.

The quartz is more dominant than the plagioclases in the matrix or groundmass possibly former glass. It is micrometric (up to 250 μm) and appears more or less flattened with undulose extinction, the plagioclases show sometimes twinning.

The clay matrix is composed of very fine-grained components which are indistinct.

6) Andalusite slate: Sample 037 E1-e

It is a dark-coloured metasedimentary rock made up of very fine grains not identifiable with the naked eye or with a magnifying glass (**Figure 5(c)**) which alternates with light medium-grained (**Figure 5(e)**) and fine-grained rocks (**Figure 5(g)**) identified respectively as feldspathic metagreywacke and feldspathic metasiltstone.

Under the microscope the rock presents a foliated texture outlined by the orientation of elongate altered andalusite in very fine dark grained indistinct matrix (**Figure 5(d)**).

7) Feldspathic metagreywacke: Sample 037 E1-e

Under the microscope, the medium-grained light layer of the sample shows a more or less oriented granoblastic texture (**Figure 5(f)**). It is made up of abundant quartz grains and feldspar dispersed in a very fine-grained matrix composed of quartz, plagioclases, calcite, and opaque minerals.

Quartz of micrometric size (up to 850 μm) contains many fluid inclusions. It presents variable shapes (subrounded, subangular, stretched), and shows often an undulose extinction. It is in monocrystalline dominant form, or secondarily in a polycrystalline form. The plagioclases are also micrometric (up to 600 μm). They are heavily altered, partly or completely recrystallized but the residual grains are still recognizable by their characteristic twins.

The matrix contains very fine-grained quartz and feldspars. Subordinate minerals are represented by epidote, sericite, calcite, and opaques (well disseminated) minerals. All of these minerals are micrometric in size.

8) Feldspathic metasiltstone: Sample 037 E1-e

Under the microscope, the fine-grained light layer of the sample shows a more or less oriented granoblastic texture (**Figure 5(h)**). It is made up of abundant quartz grains and subordinate feldspar, both are dispersed in a very fine-grained matrix composed of indistinct quartz and plagioclases, epidote, sericite and leucoxene.

The clasts of quartz are micrometric in size and reach rarely 100 μm. They present variable shapes (subrounded, subangular, stretched), and show often an undulose extinction. The plagioclases are smaller than quartz, they are often inferior to 70 μm. Some of the clasts are still recognizable by their twining.

The dominant very fine-grained matrix contains indistinct quartz and feldspars. Subordinate minerals are epidote, sericite, leucoxene.

4.1.2. Quartz Veins

Numerous quartz-feldspar veins occur within the altered metavolcano-sedimentary

rocks and plutonic intrusive rocks of the open-pits as well on the drill cores. Their dimensions vary in width and length, from millimetre to centimetre in width and from centimetre to decimetre in length. In the open-pits, their length can reach 3 m. Their contacts with their hosts are clear and they are occasionally interconnected.

1) Brecciated quartz-feldspar vein: Sample 576 E1-d

It corresponds to a filling of fracture of intrusive rock by brecciated quartz-feldspar vein (Figure 6(a)).

Under the microscope, the rock shows a granoblastic texture marked by an association of quartz and plagioclases in a minor poorly sorted matrix of micrometric size (Figure 6(b))

The quartz is anhedral, micrometric to millimetric (up to 4 mm), highly strained with undulose extinction. It is also cloudy because of the great numbers of fluid inclusions. The Plagioclases crystals are subhedral with a micrometric to millimetric size (up to 1.8 mm). They show both simple and multiple twins, the twins are occasionally bended. Some of the plagioclases are partly recrystallized.

The matrix is composed of rare micrometric chlorite, sericite and epidote.

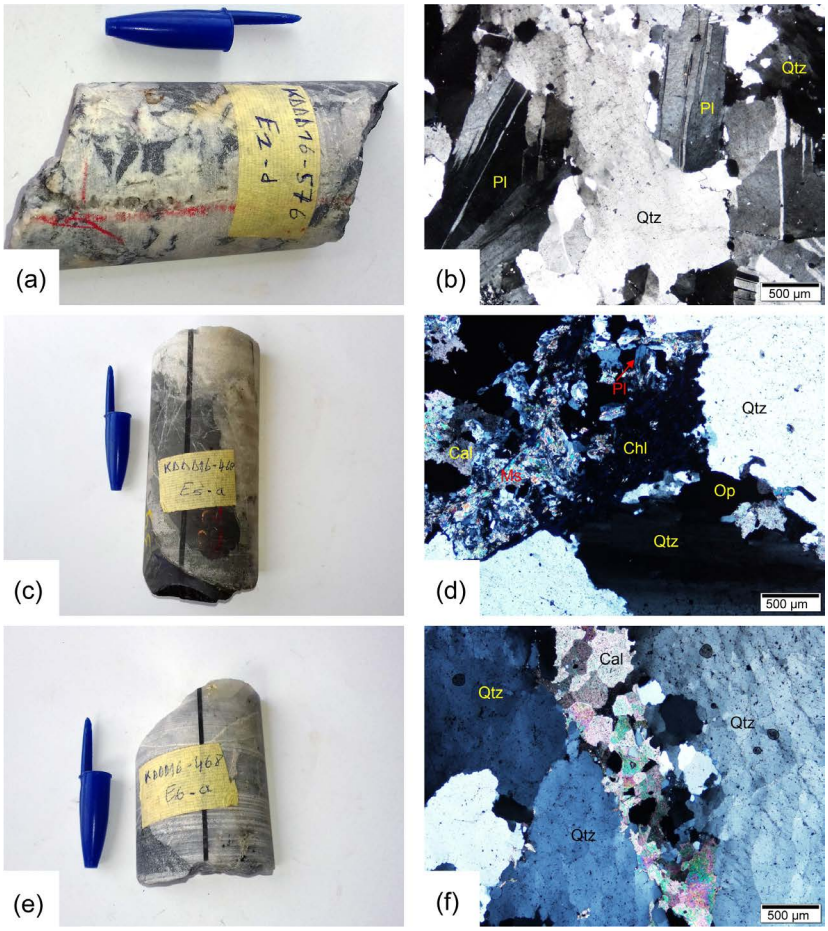

Figure 6. Macroscopic and microscopic pictures of the quartz vein arrays. (a) and (b) Brecciated quartz-feldspar vein. (c) and (d) Sulphide-bearing chlorite-quartz vein. (e) and (f) Quartz-carbonate vein.

2) Sulphide-bearing chlorite-quartz vein: Sample 468 E5-a

It is a filament of milky-white quartz, made up mainly of quartz veinlets, sulphides, chlorites and carbonates, observable with the naked eyes (Figure 6(c)).

Under the microscope the vein shows a granular texture formed mainly by the spectacular development of sutured crystals of quartz in a matrix composed of quartz, plagioclases, chlorite, calcite, sericite, epidotes and opaque minerals (Figure 6(d)).

The dominant crystals of quartz are millimetric and may exceed 5 mm in length. They are anhedral, sutured and strained. They expose undulose extinction and occasionally some subgrains. The phenocrystals of plagioclases are micrometric, up to 600 μm and subhedral.

Calcite has variable shape; it occurs in free form or in an aggregate of grains which cut the crystals of quartz. This shows its late character compared to quartz. The chlorite has a dark blue interference colour in crossed-plane polarized. It is associated with sericite, epidote, sulphides and carbonates.

3) Quartz-carbonate vein: Sample 468 E6-a

It is a milky-white vein, composed mainly of quartz and carbonates (Figure 6(e)).

The rock shows a granular texture under the microscope and displays dominant quartz in a matrix composed of quartz, carbonates, and rare muscovite (Figure 6(f)).

Quartz is micrometric in size and occurs as anhedral strained crystals which display undulose extinction or subgrains.

The matrix is poorly sorted with dominant micrometric grains of carbonates which intersect or grow between the quartz.

4.1.3. Plutonic Rocks

1) Tonalite: Sample 468 E2-c

The tonalite is a leucocratic rock with a granular texture (Figure 7(a)).

Under the microscope, the rock presents a granular porphyritic texture, consisting of altered phenocrysts of plagioclases, quartz, amphibole and biotite dispersed in recrystallized groundmass of feldspar, quartz, amphibole, biotite, chlorite, epidote, calcite, rutile and opaque minerals (Figure 7(b)). The inequigranular matrix consists of quartz, plagioclases, biotite, chlorite and calcite.

The plagioclases phenocrysts are elongated and heavily altered. They vary in size (approximately 1 to 2.5 mm) and are transformed in a mixture of feldspar, quartz, sericite, chlorite, opaque and epidotes. The feldspars present in the groundmass are micrometric and granular. The quartz occurs in the form of anhedral grains of micrometric size (50 to 450 μm). The amphibole is generally retromorphic, biotite is brown, micrometric in size (200 to 400 μm).

Chlorite occurs in micrometric size (200 to 920 μm) with varying shapes. Some individuals show an elongated subhedral form. Chlorite is weakly pleochroic in the shades of light green. It pseudomorphosed both amphibole and biotite. Calcite is anhedral and granular; its size varies between 60 to140 μm. It intersects the chlorite and therefore appears to postdate it.

The accessory minerals are rutile and leucoxene.

2) Microtonalite: Sample 037 E2-a

It is a leucocratic rock with a fine-grained structure. It is made up of visible dark chlorite and light feldspars (**Figure 7(c)**).

Under the microscope, the rock presents a porphyritic microgranular texture, consisting of relics of weathered plagioclases, dispersed in a recrystallized matrix of plagioclases, quartz, epidote, chlorite, calcite, zircon, leucoxene, and opaque minerals (**Figure 7(d)**).

Residual plagioclases are completely altered; alteration gives a mixture of chlorite, sericite, epidote. Some phenocrysts show occasionally twining which allow them to be identified.

The matrix of the rock is composed of plagioclase, quartz, chlorite, epidote and opaque minerals. The plagioclases vary in size (50 - 300 μm); many of them are euhedral and show a twining, some of them form an association in a cluster that looks like a bouquet of flowers. Chlorite occurs in the form of small aggregate grains of micrometric size (<50 μm). It invades and pseudomorphoses massively a former crystal which could be amphibole. Opaque minerals are abundant and dispersed in the micrometric matrix. The calcite shows poorly crystallized grains but it still identifiable by its high birefringence and by the presence of cleavages on the well-formed sections. Epidote is often seen with chlorite.

The accessory minerals are zircon and leucoxene.

3) Quartz diorite: Sample 466 E2-d

The rock is mesocratic, fine-grained; it is made up of quartz, plagioclases, amphibole and biotite, all visible to the naked eyes (**Figure 7(e)**).

The rock shows a porphyritic granular texture (**Figure 7(f)**) with a dominant plagioclases, amphibole and biotite.

The plagioclases are altered and micrometric, up to 900 μm. The alteration obliterates their original form; it gives a mixture of white mica (sericite) and epidote. Very rare phenocrysts show twining. No K-Feldspar has been observed. The amphiboles are micrometric to millimetric (up to 3 mm), prismatic or elongate, free or in aggregate. They are pleochroic from pale to green pale and develop on quartz and plagioclases. Biotite is micrometric to millimetric (up to 1 mm), brown-coloured and occurs as subhedral, it replaces locally amphibole.

The recrystallized matrix of the rock is formed mainly of quartz, plagioclase, biotite, calcite chlorite, epidote, apatite and opaque minerals. Quartz is micrometric; it presents xenomorphic form and shows discrete undulose extinction. Chlorite is also micrometric and has variable forms; it pseudomorphoses both amphibole and biotite.

The accessory minerals are apatite and opaques; apatite in elongated (up to 1.5 mm) or hexagonal sections (up to 230 μm).

4) Quartz diorite: Sample 466 E1-c

It is a dark coloured rock, medium-grained with a granular porphyric texture (**Figure 7(g)**). The facies are cut by carbonate veins and locally contains carbonates in the matrix.

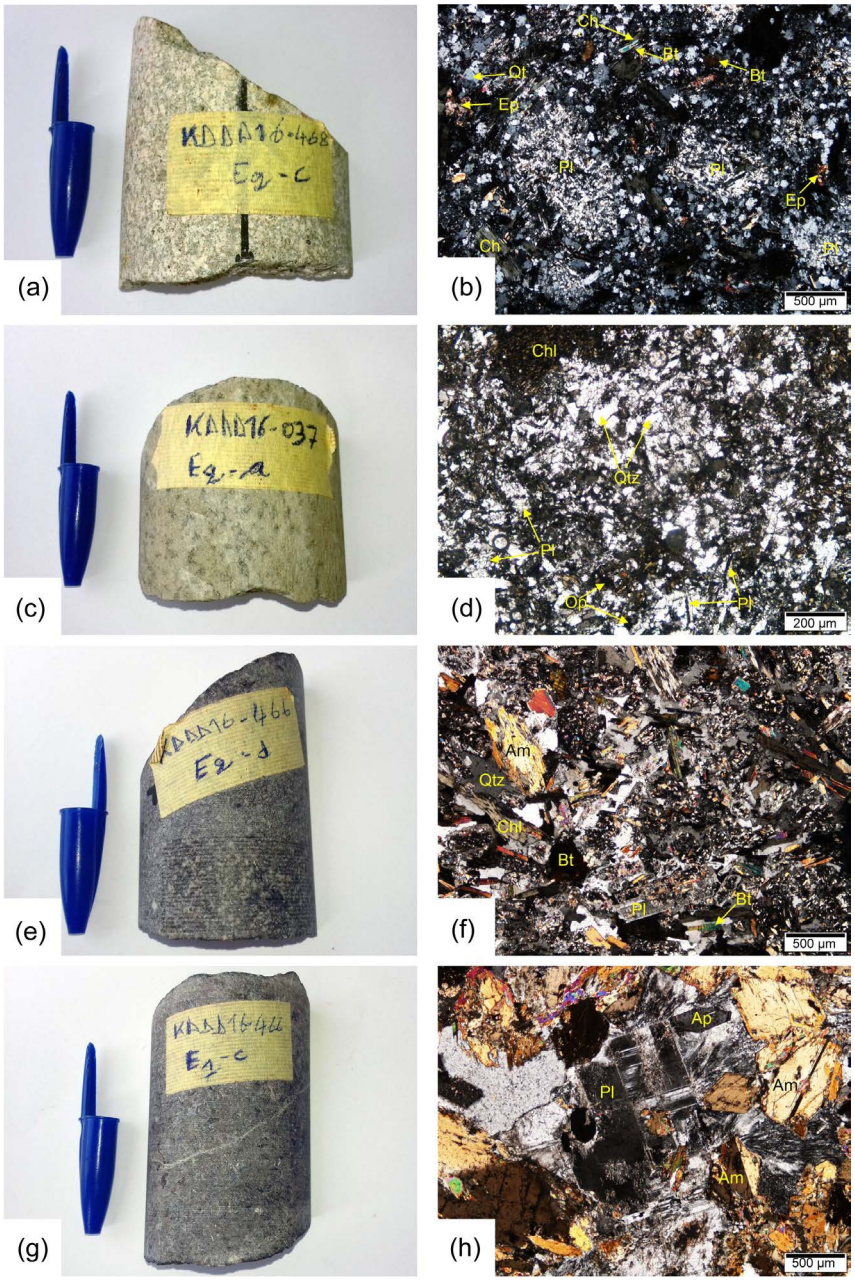

Figure 7. Macroscopic and microscopic pictures of the plutonic rocks. (a) and (b) Tonalite. (c) and (d) Microtonalite. (e) and (f) Quartz diorite. (g) and (h) Quartz diorite.

Under the microscope, the rock consists of phenocrysts of plagioclases, amphiboles and biotite dispersed in a recrystallized matrix (**Figure 7(h)**).

Plagioclases are heavily altered and give a mixture of sericite and epidotes. The weakly damaged crystals show a millimetric size up to 2.3 mm. The older phenocrysts are generally replaced by new grains of plagioclases largely present in the matrix. Amphiboles are micrometric to millimetric (0.6 - 3.5 mm), and slightly pleochroic in the brown tones. The phenocrysts are in elongated or hexagonal prismatic form. The elongated crystals could attain 3.5 mm. Both are twinned and pseudomophosed locally by biotite. Quartz is micrometric to mil-

limetric (up to 1.3 mm), it shows undulose extinction. Biotite is micrometric to millimetric, up to 2.2 mm, and subhedral. It is brown in plane-polarized light and it contains a lot of needle-like rutile inclusions. Locally, it is pseudomorphosed by chlorite which takes its form. Chlorite is in association with epidotes and rutile.

The rock matrix is essentially formed of quartz, relics of older plagioclase, chlorite, calcite, epidote, opaque minerals.

The other accessory minerals are apatite, rutile, and opaque minerals. Apatite is the dominant accessory mineral. It is in the form of elongated euhedral prismatic crystals or in a hexagonal section. The elongated crystals are micrometric to millimetric, up to 1.5 mm.

4.2. Stratigraphic Column

The laterite forms a width crust which prohibit any observations on the outcrops, the stratigraphic column proposed here have been identified on the basis of the study of a representative hole (KDD16-470) of cores drilling (**Figure 8**). The hole is deep to 350 m, and dips steeply to the NE (50˚), it is perpendicular to the metavolcano-sedimentary rocks.

The rocks of the FGD are organized from top to bottom towards the protolith into several units: lateritic duricrust, saprolite, saprock and unweathered rocks.

Duricrust occupies the top of the stratigraphic column; it is indurated and enriched with iron. It forms parts of deep-weathering profiles. Its thickness is 3 meters.

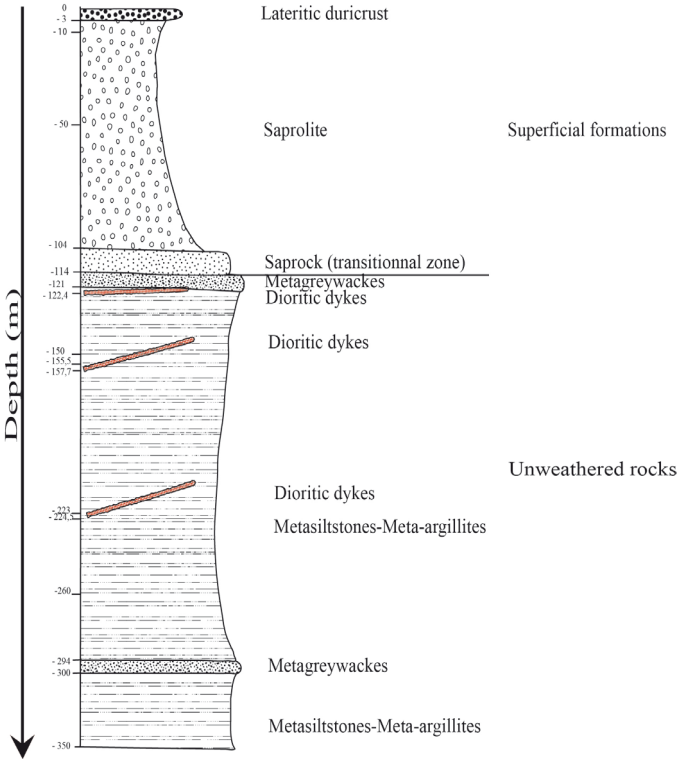

Figure 8. Stratigraphic column of the Faboula Gold deposit.

Saprolite is intercalated between duricrust and bedrock; it has an extension superior to 50 m. It constitutes a horizon of deep weathering of the protolith where the primary minerals are totally destructed and transformed in muds, oxides, or hydroxides. The intensity of the alteration masks the framework of the protolith.

Saprock is a transitional horizon between saprolite and protolith, it has an extension of ten meters. In the saprock unit the minerals are partially decomposed, allowing the identification of the bedrock.

Duricrust, saprolite and saprock constitute the superficial formations; they are in part the result of weathering of the Paleoproterozoic bedrock.

Unweathered rocks are at the bottom of the stratigraphic column where the fabrics of the rocks are preserved. The petrographic and microstructural studies have been carried out on samples taken in this horizon. They are constituted by an alternation of metasiltstones, meta-argillites and slates with subordinated metagreywackes. The rocks contain various quartz veins, some of them are mineralized with visible gold. These veins are locally enriched by calcite, chlorite and sulphide; there are also levels of disseminations of sulphides in the rocks. The protolith is affected by hydrothermal alteration.

At certain levels, (from 121 to 122.4 m; from 155.5 to 157.7 m; from 223 to 224.5 m), the metasiltstones, meta-argillites and slates are intersected by dykes of dioritic composition.

This stratigraphic column gives the relative lithostratigraphic succession of the deposit and constitutes a good step in our knowledge of the subsoil of the deposit and beyond southern Mali.

4.3. Structures

The analysis of the structural data collected in this study allowed us to identify the structural characteristics of the deposit in the open-pits (main zone and zone 5) as well as on the drill cores. Structural features as well as foliation, en-echelon tension gashes, faults and fractures have been recognized. These deformations are ductile, ductile-brittle and brittle. The overall tectonic scheme identified and characterized for the first time for the deposit is then replaced in the Eburnean orogeny framework of the Leo-Man Shield.

4.3.1. Ductile Deformation

The rocks of the FGD exhibit steeply dipping foliation, the main marker of this deformation is the foliation-S1. In the open-pits, it developed remarkably in the fine-grained facies on the west side. The foliation-S1 has been identified and measured in the open-pits (N = 195) and on the drill cores (N = 40). In both cases, it is parallel to the stratification-S_0 (**Figure 9(a)** and **Figure 9(b)**). This parallelism defines an S_0 - S_1 composite surface which trajectories are fairly homogeneous in the open-pits and on the drill cores. In either case, it strikes between N130˚ and N180˚. Its dip direction fluctuates between SW to W and its values range from 50˚ to 90˚ (**Figure 10** and **Figure 12**). On average, S_0 - S_1

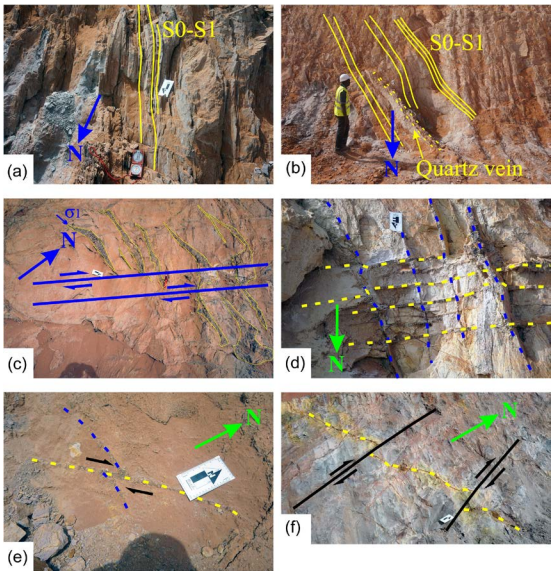

Figure 9. Some structural features observed in the open-pits of the deposit. (a) and (b) Altered metavolcano-sedimentary rocks with a composite surface S_0 - S_1. (c) An en-echelon sigmoidal tension gashes indicating a shear zone with dextral movement in the NE-SW direction. (d) Two sets of quartz vein arrays (showing mutual intersection indicating their contemporaneity. (e) An NE-SW quartz vein shifted in a dextral movement by an E-W quartz vein. (f) Dextral thrust fault intersecting an NE-SW quartz vein.

strikes NNW-SSE and dips steeply towards the WSW. It is the major deformation of the deposit.

A stretched quartz and andalusite have been identified respectively on thin sections of the quartzofeldspathic and andalusite schists (**Figure 4(h)** and **Figure 5(d)**). They are probably carried by the foliation plane. Both are interpreted as a result from the same ductile deformation.

4.3.2. Ductile-Brittle Deformation

In the FGD, there are two types of bodies of minerals which have been precipitated into the fracture within rocks: 1) en-echelon tension gashes, 2) and a quartz vein arrays. The former marks the ductile-brittle deformation recognized in the deposit.

The tension gashes are organized en-echelon, some of them are curveted (**Figure 9(c)**). They have been observed locally at the west side of the main open-pit at its level 365 m. They extend to the length of 1.4 m, with an opening of a few cm thick (7 - 20 cm). In the open-pits, shear fabrics indicate dextral movement in the NE-SW direction (**Figure 9(c)**).

The quartz vein arrays have been observed and measured in the open-pits (N = 187) as well on the drill cores (N = 42). They intersect all the lithologies of the deposit and seem to be later. The quartz vein arrays have a millimetric to centimetric thickness and rarely reach the meter. However, locally in the open-pits, some veins show a length varying between 1 and 3 m. In the open-pits two sets of quartz vein arrays are secant on the S_0 - S_1 surface (**Figure 9(d)** and **Figure 9(e)**), while one is parallel to it (**Figure 9(b)**). On the drill cores, quartz-carbonate

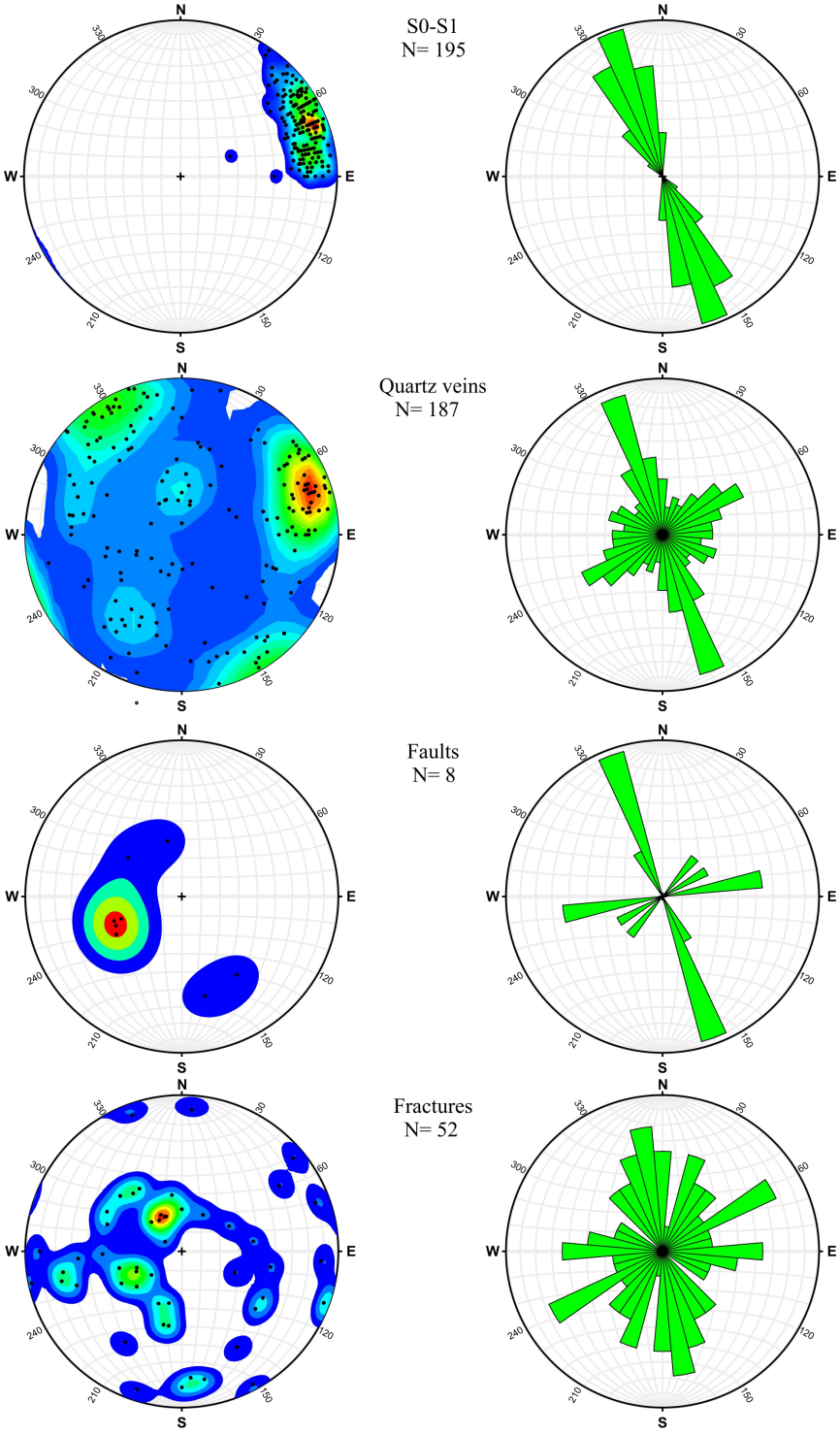

Figure 10. Stereograms of densities of poles and rose diagrams from the structural features measured in the open-pits of the deposit.

veinlets are observed parallel to the S_0 - S_1 and microfolding affects them (**Figure 11**).

The measurements of the orientation of the quartz vein arrays shows three sets of populations (**Figure 10** and **Figure 12**):

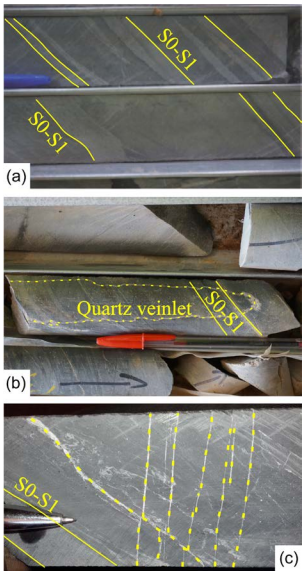

Figure 11. Some structural features observed on the drill cores of the deposit. (a) Composite surface S_0 - S_1. (b) Microfolded veinlet intersecting S_0 - S_1. (c) Two sets of veinlets with one intersecting clearly S_0 - S_1.

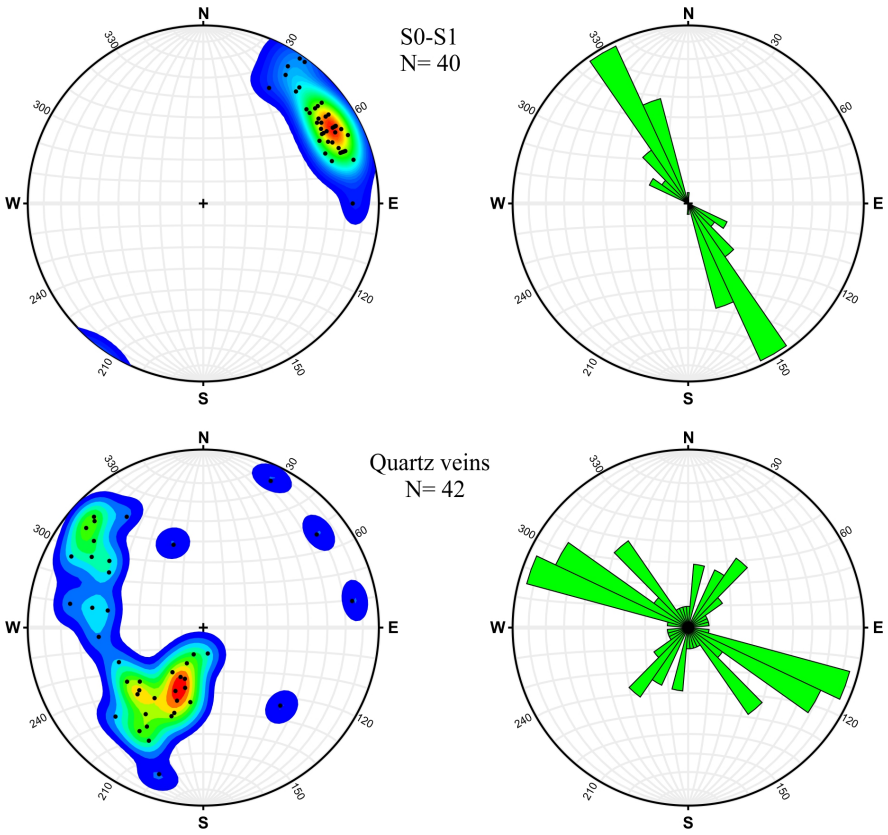

Figure 12. Stereograms of densities of poles and rose diagrams from the structural features measured on the drill cores of the deposit.

✓ a first set of population named QV_1: it strikes N140 to N180 (NW-SE to N-S) and dips steeply (50˚ - 80˚) towards the SW or W;

- ✓ a second set of population labelled QV_2: it strikes N40 to N80 (NE-SW to ENE-WSW) and dip more steeply (65˚ - 85˚) towards the SE, NW or SSE;
- ✓ a third set of population designated QV_3 with an E-W trending and a dip varying between 6˚ to 70˚ towards the S or N.

Some shifts between the quartz vein arrays have been observed locally in the open-pits, in particular between QV_2 and QV_3, the latter being shifted in a dextral movement. However, most of veins crosscut each other; they seem to be contemporaneous, even if field observations do not allow an obvious relative chronology to be established between the three sets of populations. The most mineralized veins show an NE-SW trending with a dip toward SE [71].

4.3.3. Brittle Deformation

It is marked by faults and fractures which have only been observed and measured in the open-pits (**Figure 9**). They display several directions; some of them are sub-parallel to the S_0 - S_1, others are totally sequent.

Structural analysis of the trending of the faults shows two (2) main directions (**Figure 10**):

- ✓ NNW-SSE trending with a shallow dip to the ENE;
- ✓ ENE trending with a shallow dip to the SSE.

The NNW-SSE faults correspond to reverse faults while the ENE directions seem to be linked to a shear zone.

The fractures show late characters, they cut the quartz vein arrays. Analysis of the density of the poles of the fractures does not show any preferential orientation on the stereogram, and on the rosette (**Figure 10**).

5. Discussion

5.1. Lithostratigraphic and Intrusive Units of the FGD

The FGD lithostratigraphic context is dominated by an alternation of fine to very fine-grained metavolcano-sedimentary rocks with subordinated clastic medium-grained facies; all are of Paleoproterozoic age. They are made of metagreywackes, metasiltstones, meta-argillites, slates and schists. This sequence represents a flysch type unit. The sequence is intersected by small dioritic bodies, as well as tonalitic dykes; granitic and monzonitic rocks (**Figure 3**) have been reported by [68] but we did not identify them in the open-pits or the drill cores. Despite the fact that there is no geochronological data on the deposit, we can assume that the sedimentation occurred between 2125 Ma and 2092 Ma, if we compared it to what is known in the adjacent and neighbouring areas of Siguiri and Massigui. In the Siguiri basin, sedimentation took place between ca. 2124 ± 7 Ma and 2092 ± 5 Ma [38]; a period similar (ca. 2125 ± 8 Ma - 2092 ± 7 Ma) to that of the sedimentation of the Massigui region recognized by [15].

In the sample 579 E1-a, the boundaries between the crystals of polycrystalline quartz are occasionally sutured. This is generally a characteristic of quartz from metamorphic sources. The fragment with plagioclase laths dispersed in a fine-grained altered matrix of the same sample is probably a volcanic rock fragment.

A volcanic origin has been also found on the sample 468 E4-a whose quartz shows locally straight edges; this quartz seems to develop from well-developed phenocrystal a characteristic of volcanic quartz.

The Sample 468 E4-a contains quartz with locally straight edges; it seems to develop from well-developed phenocrystal; this characteristic suggests that it could have a volcanic origin. This sample contains amphibole too; this mineral is generally part of the paragenesis of metamorphosed sedimentary rocks with basic protoliths. From this observation, we consider that the protolith of the sample 468 E4-a, which is a metagreywacke, would initially be magmatic. For this reason, it has been identified as an amphibole bearing volcanoclastic metagreywacke.

The study of the mineralogical assemblages of the matrix of metavolcano-sedimentary rocks indicates that all the rocks have been metamorphosed under conditions close to the greenschist facies. However, some facies show a paragenesis with actinolite, epidote, biotite, plagioclase, and quartz, which suggests that they have reached the epidote-amphibolite facies. In addition, there are features indicating that the rocks of the deposit have experienced hydrothermal events as shown by the numerous quartz veins arrays and the blue interference from chlorite in the sample 468-E5a. The hydrothermal alterations are also highlighted by the processes seen in the thin sections such as silicification, carbonation, sulphidation, chloritization and sericitization, etc.

Locally, a fine-grained volcano-sediment is transformed into andalusite granofels (sample 464 E2-b), due to the contact metamorphism generated by the emplacement of an intrusive rocks. However, the sample 037 E1-e identified as an andalusite slate presents a foliation materialized by the stretching of the andalusite porphyroblasts. This andalusite slate could be the product of a regional metamorphism that affected the andalusite granofels. Therefore, the rocks of the deposit show a history inherited from contact metamorphism and regional metamorphism; the contact metamorphism seems to be prior to the regional metamorphism.

The various origins of the sediments highlighted by this work implies the destruction of an ancient, exposed crust in a volcanic environment who contributed to the production of clasts of volcanic origin for the sedimentation which could be contemporaneous with volcanism. Afterwards, these rocks will be deformed and metamorphosed in a local and regional setting. They underwent tectonic tightening that affected the region at the closure of the basin.

The stratigraphic column of the FGD described for the first time in a publication essay shows the volumetric importance of metasiltstones and meta-argillites. These rocks could be related to a volcanoclastic origin since the fine-grained volcanoclastic rocks commonly altered into clay are often classified as shales [72].

The FGD possesses similarities with the Kalana gold deposit, where metavolcano-sedimentary rocks, represented by pelites, tuffaceous sandstones, sand-

stones, siltstones and microconglomerate, are intersected by dioritic rocks and dioritic, tonalitic and andesitic dykes [69] [73].

The Faboula gold deposit presents a lithostratigraphic context similar to that of many Birimian basins of the Leo-Man Shield despite some differences noted here and there. For example, it shares some resemblances with the formation of Balato of the Siguiri basin described by [38]. According to these authors the formation is dominated by dark grey to light grey massive siltstones beds grading upwards to shales, alternating with cm-thick shale-siltstones and rare fine greywackes interbeds.

5.2. The Structural Features

A detailed analysis of the structural data collected, in the open-pits and on the drill cores, allows us to discriminate several types of deformation which have folded and sheared the metavolcano-sedimentary rocks of the FGD. Their signatures are typical of ductile, brittle-ductile and brittle deformations. They have been integrated into the overall tectonic scheme described for the northwestern margin of the Leo-Man Shield, particularly in its Malian and Guinean parts [15] [49] [74] [75].

5.2.1. The Ductile Deformation

The first stage of deformation is ductile. It is characterized by structural features developed only in the metavolcano-sedimentary rocks and include mostly NNW-SSE foliation trending. It is marked by the parallelism between schistosity and stratification which suggests an isoclinal folding context. It is responsible for the crustal thickening of the metavolcano-sedimentary rocks and is linked to a compression event-oriented ENE-WSW. It is the major deformation of the deposit and it has a regional extent.

Similar striking of S_0 - S_1 have been reported for the Kalana gold deposit with however opposite dipping direction [69] [73]. The opposition of the dip directions of S_0 - S_1 at Faboula and Kalana suggests that the two deposits are located on either side of a syncline where the Kalana area occupies the western limb of the fold and the Faboula the oriental one. This assertion is in line with the analysis of the attitude of the tension gashes observed in the two deposits.

Across the WAC, isoclinal folding has been described. In the near ca. 2125 - 2090 Ma Bagoé basin, composite surface S_0 - S_1 has been reported by [15]. According to these authors, it presents similar strike (NNW-SSE) but dips steeply towards the ENE at the Bagoé Bridge, outside the village of Niamala and in the Banifing River. In the adjacent ca. 2115 - 2090 Ma Siguiri basin NNW-SSE oriented folds, due to ENE-WSW compression, have been described by [49].

5.2.2. The Ductile-Brittle Deformation

This stage is poorly expressed in the field. It has been identified through the interpretation of the sigmoidal en-echelon tension gashes filled by quartz. Its extent remains unclear, and there is no evidence of the presence of a large regional

shear zone in the deposit.

The development of the tension gashes is related to the stress field underwent by the rocks when they were buried. It is well known that sigmoidal gashes are related to shear zones which develop at an acute angle (45˚) to the direction of maximum compressive stress given by the tip of the gashes. In the deposit, the curvature of the sigmoidal gashes indicates a dextral movement in the NNE-SSW direction which results from an ENE-WSW regional shortening.

In the Kalana deposit, a set of sinistral sigmoid tension gashes related to an ENE-WSW compressive stress has been identified by [76]. The opposition between the kinematics of shearing at Faboula and Kalana suggests that these two deposits are located on opposite limbs of the same fold as evidenced by the similar strike of S_0 - S_1 and its opposite dip direction.

At the scale of southern Mali and the Leo-Man Shield, shearing has also been described from neighbouring NNE-SSW Siekorolé dextral shear zones [77] and the NE-SW to NNE-SSW Banifing sinistral Shear Zone in the Bagoé basin [3] [15] [62] [74] [75]. In the bordering Siguiri basin, at its southern edge not too far from the FGD ductile deformation along sinistral faults occurred after the crystallization of the granodiorites, around 2.08 Ga [8]. These authors related it to a Late Eburnean ENE-WSW shortening. Further in the south, sinistral shearing has also been reported for the Sassandra Shear Zone at the border of the Archean of Kénéma-Man and the Birimian of Baoulé-Mossi domain [55].

Numerous quartz vein arrays show three different orientations within the FGD. One type (NW-SE to N-S) is parallel to the regional composite surface S_0 - S_1, while two others (NE-SW to ENE-WSW and E-W) crosscut it. Quartz veins arrays have been reported in the Kalana gold deposit; they are controlled by the intrusive granitic rocks [78].

According to [73], there are two groups of quartz veins crosscutting a bedding-parallel schistosity surface, striking N170 and dipping steeply towards the E: 1) a first set of groups which show more irregular measured strikes, roughly N-S but some of them are oriented NE-SW and others E-W; 2) a second set of groups, more homogeneous than the other, with closely spaced veinlets striking NE-SW. Both are coeval according to the authors, a point of view shared by Kusters [76] and [78]. The latter suggested that there are many parallel veins, stacked on top of each other, due to their different strikes and dips, some of them must cross and cut each other.

According to [70], the gold mineralization of the Faboula deposit occurs in the form of free gold and is associated with NE- SW quartz veins steeply dipping to SE, which in this study corresponds to the second set of population labelled QV_2. A major phase of mineralization commonly associated with quartz veining during a D_3 deformation linked to WSW-ENE shortening and formation of the dextral Siekorole shear zone is described by [77]. In the neighbouring Siguiri basin, gold mineralization is associated with one main and, at least, three minor sets of auriferous quartz veins; the main quartz-vein set shows remarkably con-

sistent easterly to northeasterly trends and steep southerly to subvertical dips throughout the Siguiri Mining Complex [79]. In the Siguiri Gold District, gold-bearing mineral occurrences are formed along subvertical N-S reverse faults, NE-trending dextral shear zones, WNW-trending sinistral faults, and E-trending normal relay faults developed or reactivated early-D_3 [49].

5.2.3. The Stage of Brittle Deformation

The brittle deformation is linked to the late emplacement of faults and fractures. Fractures are present in number in the area, their measure show that they are randomly oriented. They disrupt the main S_0 - S_1 and the quartz vein arrays and are clearly post faulting. Faults are more regularly oriented than the fractures. They show orientation similar to the most important attitudes seen in the quartz veins arrays: NNW-SSE and ENE-WSW. The NNW-SSE faults correspond to reverse faults while the ENE directions seem to be linked to a shear zone. They could mark the continuation of the brittle-deformation or they might be a result of a concomitant event developed during a compressive event.

5.2.4. Global Tectonic Context of Folding and Shearing

In the Faboula gold deposit, there is an association of ductile, brittle-ductile and brittle deformations. The essential question is whether these deformations belong to different phases or are they the result of a progressive deformation starting with the ductile type and ending with the brittle type?

The sequence of deformations recognized in the deposit shows a ductile deformation marked by isoclinal folding developed during an ENE-WSW compression event which is also at the origin of a brittle-ductile deformation whose sigmoidal en-echelon tension gashes indicate a dextral movement in the NNE-SSW direction. Thus, the folding and the shearing are related to the same greatest compressive stress $\sigma 1$. The brittle ductile-deformation is localized in the limb, its whole data set (tension gashes, reverse faults, strike slip faults) is consistent with Riedel's shear structures developed in a compressive regime; the orientations of the faults are in accordance with the R and R' structures.

This type of deformation with folding and shearing, related to the same ENE-WSW compressive stress, could occur simultaneously during a transpressive mechanism. Our interpretation is supported by the fact that the reverse faults strike perpendicular to the main compressive stress $\sigma 1$ in the same direction as the folds and foliation. Indeed, transpression is a combination of strike-slip faulting, thrust-reverse faulting, and folding [80]. It is the spectrum of combinations of strike-slip and coaxial strain involving shortening perpendicular to the zone [81]. Transpression is commonly associated with oblique plate convergence.

Due to its characteristics, and also because it corresponds more to the D_2 or D_3 than the D_1 tectonic phases, at the scale of the Leo-Man Shield, we will call it D_{2Fb}. Indeed, no relic of a first tectonic phase D_1 has been identified in the deposit, even if a first ductile event marked by cryptic tight recumbent folds linked to

N-S compression, was recognized by [49] in the adjacent District of Siguiri.

The transpressive dextral D_{2Fb} highlighted at Faboula could be equivalent to the regional D_2 or D_3 deformations recognized at the scale of the Leo-Man Shield. It could be correlated with D_3 of [3], D2 of [79], D3 of [77]; D_{2S} of [49] and D_3 of [15]. All these middle phases of the Eburnean orogeny are bracketed between ca. 2115 - 2074 Ma [3] [15]. The deformation of [77] which best matches the D_{2FB} is D_3. The latter is linked to ENE-WSW shortening and the genesis of the dextral Siekorole Shear Zone associated with the development of mineralized quartz veins. In the neighbouring Massigui region, dextral D_3 is indicated by the tension gashes [3]. This phase brittle/ductile in character, is highlighted by fracture cleavage, microfaults and vein arrays; its regional fault drag patterns into the Banifing Fault Zone are consistent with a component of dextral displacement [15]. The folding and shearing associated within the D_{2Fb} are also in agreement with the D_2 of [79] which is the main deformation phase of the Siguiri Mining Complex. The D_2 deformation of this author shows N-S trending strike-slip and reverses faults anastomosing around and enveloping open-to tightly folded domains. The D_{2Fb} dextral transpressive deformation corresponds to the main and second deformation (D_{2S}) of [49], which would result from an E-W to ENE-WSW directed compressions. According to these authors, it was responsible for the generation of the dominant N-trending of the Siguiri Gold District.

The abundance of quartz veins arrays and their relationship with the deformation structures indicates probably that the mineralization is structurally controlled during a hydrothermal event. They could be related to relaxation or orogenic collapse immediately after the D_4 [77], which is a tectonic event linked with to NW-SE shortening and on-going magmatism.

6. Conclusions

This study gives a new idea of the nature and the spatial organization of the Paleoproterozoic formations of the FGD and the deformations associated with them. Drill cores, for example, revealed geological features of objects that do not appear on the surface. All this testifies to the interest of combining multiple data set in the study of Birimian terrains. The methodology we have adopted is therefore adequate in terms of geological studies for regions with strong weathering and/or strong vegetation cover.

The lithological and structural studies carried out give a general idea of the distribution of rocks and structures in the FGD. All the work, from observation to interpretation, highlights the following conclusions.

- ✓ The FGD is affected by intense weathering up to a depth of 90 m which makes it difficult for any geological study.
- ✓ The field and petrographic studies indicated that the metavolcano-sedimentary rocks are essentially very fine to fine-grained quartzofeldspathic rocks with subordinated medium-grained facies. They are made up of feldspathic meta-

greywackes, volcanoclastic metagreywackes, feldspathic metasilstones, meta-argillites and schists. These rocks are intruded by plutonic rocks of intermediate composition (tonalitic and dioritic). The lithologies are intersected by en-echelon sigmoidal tension gashes filled with quartz and quartz vein arrays which composition are quartzofeldspathic, associated with carbonates and sulphides and free gold.

- ✓ The mineralogical assemblages of the metavolcano-sedimentary rocks show a matrix with recrystallization indicating that the rocks were metamorphosed under greenschist facies conditions and that locally the amphibolite facies was reached.
- ✓ The various origins of the sediments highlighted by this work imply the destruction of an ancient exposed crust in a volcanic environment that contributed to the production of clasts of volcanic origin for the sedimentation which could be contemporaneous with volcanism.
- ✓ The stratigraphic column revealed that the deposit is hosted by a sequence of very fine to fine-grained metavolcano-sedimentary rocks with subordinated medium-grained metagreywackes. This sequence could be related to the thickening of the lithostratigraphic units.
- ✓ The main structural characteristics of the Faboula gold deposit point out several stages of deformation combining a ductile and a ductile-brittle type which then evolve into a brittle type. The ductile and ductile-brittle types exhibit a combination of folding and shearing. They are illustrated by isoclinal folds associated with an axial planar foliation, reverse faults, both oriented NNW-SSE, and dextral shear zones, underlined by en-echelon sigmoidal tension gashes filled by quartz. The curvatures of the latter indicate a dextral movement in the NNE-SSW direction which results from an ENE-WSW regional shortening. The overall orientation and kinematics of the folds, thrust faults and shears suggest that the deposit was affected by the dextral transpressive phase labelled here D_{2Fb} in comparison to the D_2 identified and described on the scale of the Leo-Man Shield.
- ✓ There is an abundance of quartz vein networks. Their relation to the structural features indicates probably that the mineralization is structurally controlled during hydrothermal events linked certainly to the circulations of fluids during the transpressive event D_{2Fb}.

In the light of the results obtained during this study, the FGD remains interesting for even more in-depth studies in order to update the typology of this deposit compared to others located in the south of Mali and even in WAC.

In terms of perspective, it would be interesting to focus future work on updating the lithological data from the drill cores and the pursuit of structural studies in order to propose a reliable geological model of the subsoil given the significant lateritic cover. This work will naturally have to be done with the interpretation of geophysical data. This will facilitate the understanding of the deposit and will undoubtedly promote its better exploitation.

Acknowledgements

This study was initiated as part of the end of study project of Master in Applied Geology of [82], at the Faculty of Sciences and Techniques (FST) of the University of Sciences, Techniques and Technologies of Bamako (USTTB). In addition, we thank the Wassoul'Or Company for accepting Mr OUOLOGUEM to carry out his end-of-study project internship, as part of the cooperation between the FST and the company, while taking in charge his stay on the mining site as well as the sponsoring of the polished thin sections used in this study.

Conflicts of Interest

The authors declare no conflicts of interest regarding the publication of this paper.

References

[1] Abouchami, W., Boher, M., Michard, A. and Albarede, F. (1990) A Major 2.1 Ga Event of Mafic Magmatism in West Africa: An Early Stage of Crustal Accretion. *Journal of Geophysical Research*, **95**, 17605-17629. https://doi.org/10.1029/JB095iB11p17605

[2] Leube, A., Hirdes, W., Mauer, R. and Kesse, G.O. (1990) The Early Proterozoic Birimian Supergroup of Ghana and Some Aspects of Its Associated Gold Mineralization. *Precambrian Research*, **46**, 139-165. https://doi.org/10.1016/0301-9268(90)90070-7

[3] Liégeois, J.-P., Claessens, W., Camara, D. and Klerkx, J. (1991) Short-Lived Eburnean Orogeny in Southern Mali. Geology, Tectonics, U-Pb and Rb-Sr Geochronology. *Precambrian Research*, **50**, 111-136. https://doi.org/10.1016/0301-9268(91)90050-K

[4] Boher, M., Abouchami, W., Michard, A., Albarede, F. and Arndt, N.T. (1992) Crustal Growth in West Africa at 2.1 Ga. *Journal of Geophysical Research*, **97**, 345-369. https://doi.org/10.1029/91JB01640

[5] Hirdes, W., Davis, D.W. and Eisenlhor, B.N. (1992) Reassessment of Proterozoic Granitoid Ages in Ghana on the Basis U/Pb Zircon and Monazite Dating. *Precambrian Research*, **56**, 89-96. https://doi.org/10.1016/0301-9268(92)90085-3

[6] Hirdes, W., Davis, D.W., Lüdtke, G. and Konan, G. (1996) Two Generations of Birimian (Paleoproterozoic) Volcanic Belts in Northeastern Côte d'Ivoire (West Africa): Consequences for the "Birimian Controversy". *Precambrian Research*, **80**, 173-191. https://doi.org/10.1016/S0301-9268(96)00011-3

[7] Egal, E., Thiéblémont, D., Lahondère, D., Guerrot, C., Costea, C.A., Iliescu, D., Delor, C., Goujou, J.C., Lafon, J.M., Tegyey, M., Diaby, S. and Kolié, P. (2002) Late Eburnean Granitization and Tectonics along the Western and Northwestern Margin of the Archean Kénéma-Man Domain (Guinea, West African Craton). *Precambrian Research*, **117**, 57-84. https://doi.org/10.1016/S0301-9268(02)00060-8

[8] Lahondère, D., Thiéblémont, D., Tegyey, M., Guerrot, C. and Diabate, B. (2002) First Evidence of Early Birimian (2.21 Ga) Volcanic Activity in Upper Guinea: The Volcanics and Associated Rocks of the Niani Suite. *Journal of African Earth Sciences*, **35**, 417-431. https://doi.org/10.1016/S0899-5362(02)00145-8

[9] de Kock, G.S., Armstrong, A., Siegfried, H.P. and Thomas, E. (2011) Geochronology of the Birim Supergroup of the West African Craton in the Wa-Bolé Region of

West-Central Ghana: Implications for the Stratigraphic Framework. *Journal of African Earth Sciences*, **59**, 1-40. https://doi.org/10.1016/j.jafrearsci.2010.08.001

[10] Tshibubudze, A., Hein, K.A.A., Peters, L.F.H., Woolfe, A.J. and Mccuaig, T.C. (2013) Oldest U-PB Crystallisation Age for the West African Craton from the Oudalan-Gorouol Belt of Burkina Faso. *South African Journal of Geology*, **116**, 169-181. https://doi.org/10.2113/gssajg.116.1.169

[11] Block, S., Baratoux, L., Zeh, A., Laurent, O., Bruguier, O., Jessell, M., Ailleres, L., Sagna, R., Parra-Avila, L.A. and Bosch, D. (2016) Paleoproterozoic Juvenile Crust Formation and Stabilisation in the South-Eastern West African Craton (Ghana); New Insights from U-Pb-Hf Zircon Data and Geochemistry. *Precambrian Research*, **287**, 1-30. https://doi.org/10.1016/j.precamres.2016.10.011

[12] Eglinger, A., Thébaud, N., Zeh, A., Davis, J., Miller, J., Parra-Avila, L.A., Loucks, R. and McCuaig, C. (2017) New Insights into the Crustal Growth of the Paleoproterozoic Margin of the Archean Kenema-Man Domain, West African Craton (Guinea): Implications for Gold Mineral System. *Precambrian Research*, **292**, 258-289. https://doi.org/10.1016/j.precamres.2016.11.012

[13] Parra-Avila, L.A., Kemp, A.I.S., Fiorentini, M.L., Belousova, E., Baratoux, L., Block, S., Jessell, M., Bruguier, O., Begg, G.C., Miller, J., Davis, J. and McCuaig, T.C. (2017) The Geochronological Evolution of the Paleoproterozoic Baoulé-Mossi Domain of the Southern West African Craton. *Precambrian Research*, **300**, 1-27. https://doi.org/10.1016/j.precamres.2017.07.036

[14] Petersson, A., Scherstén, A., Kemp, A.I.S., Kristinsdóttir, B., Kalvig, P. and Anum, S. (2016) Zircon U-Pb-Hf Evidence for Subduction Related Crustal Growth and Reworking of Archaean Crust within the Palaeoproterozoic Birimian Terrane, West African Craton, SE Ghana. *Precambrian Research*, **275**, 286-309. https://doi.org/10.1016/j.precamres.2016.01.006

[15] Wane, O., Liégeois, J.-P., Thébaud, N., Miller, J., Metelka, V. and Jessel, M. (2018) The Onset of Eburnean Collision with the Kenema-Man Craton Evidenced by Plutonic and Volcanosedimentary Rock Record of the Massigui Region, Southern Mali. *Precambrian Research*, **305**, 444-478. https://doi.org/10.1016/j.precamres.2017.11.008

[16] Grenholm, M., Jessel, M. and Thébaud, N. (2019) Geodynamic Model for the Paleoproterozoic (ca. 2.27-1.96 Ga) Birimian Orogen of the South West African Craton. Insights into an Evoling Accretionary-Collisional Orogenic System. *Earth-Science Reviews*, **192**, 138-193. https://doi.org/10.1016/j.earscirev.2019.02.006

[17] Goldfarb, R.J., Groves, D.I. and Gardoll, S. (2001) Orogenic Gold and Geologic Time: A Global Synthesis. *Ore Geology Reviews*, **18**, 1-75. https://doi.org/10.1016/S0169-1368(01)00016-6

[18] World Bank (2019) Mali Governance of Mining Sector (P164242). Report No. PIDISDSA24173. http://documents1.worldbank.org/curated/en/525361557761330402/pdf/Project-Information-Document-Integrated-Safeguards-Data-Sheet-Mali-Governance-of-Mining-Sector-P164242.pdf

[19] ITIE (2020) ITIE Mali RAPPORT POUR L'ANNEE 2017. https://itie.ml/wp-content/uploads/2020/06/10-Projet-rapport-ITIE-Mali-2017.pdf

[20] Kennedy, Q.W. (1964) The Structural Differentiation of African in the Pan-African (± 500 my) Tectonic Episode. Annual Report, Leeds University, Institute of African Geology, Leeds, 8, 48-49.

[21] Black, R. and Fabre, J. (1983) A Brief Outline of the Geology of West Africa, the Precambrian in Lexique Stratigraphique International, West Africa: Geological Introduction and Stratigraphic Terms. Ed. Fabre, 17-26. https://doi.org/10.1016/B978-0-08-030277-5.50006-7

[22] Rocci, G., Bronner, G. and Deschamps, M. (1991) Crystalline Basement of the West African Craton. In: Dallmeyer, R.D. and Lécorché, J.P., Eds., *The West African Orogens and Circum-Atlantic Correlatives*, Springer-Verlag, Berlin, 31-61. https://doi.org/10.1007/978-3-642-84153-8_3

[23] Ikenne, M., Söderlund, U., Ernst, R.E., Pin, C., Youbi, N., El Aouli, E.H. and Hafid, A. (2017) A c. 1710 Ma Mafic Sill Emplaced into a Quartzite and Calcareous Series from Ighrem, Anti-Atlas—Morocco: Evidence That the Taghdout Passive Margin Sedimentary Group Is Nearly 1 Ga Older than Previously Thought. *Journal of African Earth Sciences*, **127**, 62-76. https://doi.org/10.1016/j.jafrearsci.2016.08.020

[24] Bessoles, B. (1977) Géologie de L'Afrique: Le craton Ouest-Africain. Mém. BRGM, France, No. 88, 403 p.

[25] Peucat, J.-J., Capdevila, R., Drareni, A., Mahdjoub, Y. and Kahoui, M. (2005) The Eglab Massif in the West African Craton (Algeria), an Original Segment of the Eburnean Orogenic Belt: Petrology, Geochemistry and Geochronology. *Precambrian Research*, **136**, 309-352.https://doi.org/10.1016/j.precamres.2004.12.002

[26] Milési, J.-P., Ledru, P., Feybesse, J.-L., Dommanget, A. and Marcoux, E. (1992) Early Proterozoic Ore Deposits and Tectonics of the Birimian Orogenic Belt, West Africa. *Precambrian Research*, **58**, 305-344. https://doi.org/10.1016/0301-9268(92)90123-6

[27] Kouamelan, A.N., Delor, C. and Peucat, J.-J. (1997) Geochronology Evidence for Reworking of Archean Terrains during the Early Proterozoic (2.1 Ga) in the Western Côte d'Ivoire (Man Rise-West African Craton). *Precambrian Research*, **86**, 177-199. https://doi.org/10.1016/S0301-9268(97)00043-0

[28] Thiéblemont, D., Delor, C., Cocherie, A., Lafon, J.M., Goujou, J.C., Baldé, A., Bah, M., Sané, H. and Fanning, C.M. (2001) A 3.5 Ga Granite-Gneiss Basement in Guinea: Further Evidence for Early Archean Accretion within the West African Craton. *Precambrian Research*, **108**, 179-194. https://doi.org/10.1016/S0301-9268(00)00160-1

[29] Thiéblemont, D., Goujou, J.C., Egal, E., Cocherie, A., Delor, C., Lafon, J.M. and Fanning, C.M. (2004) Archean Evolution of the Leo Rise and Its Eburnean Reworking. *Journal of African Earth Sciences*, **39**, 97-104. https://doi.org/10.1016/j.jafrearsci.2004.07.059

[30] Papon, A. (1973) Géologie et minéralisation du Sud-Ouest de la Côte d'Ivoire. Bureau de Recherches Géologiques et Minières, Paris, Mémoire du BRGM, 80, 284 p.

[31] Beckinsale, R.D., Gale, N.H., Pankhurst, R.J., Macfarlane, A., Crow, M.J., Arthurs, J.W. and Wilkinson, A.F. (1980) Discordant Rb-Sr and Pb-Pb Whole Rock Isochron Ages for the Archaean Basement of Sierra Leone. *Precambrian Research*, **13**, 63-76. https://doi.org/10.1016/0301-9268(80)90059-5

[32] Rollinson, H.R. and Cliff, R.A. (1982) New Rb-Sr Age Determinations on the Archaean Basement of Eastern Sierra Leone. *Precambrian Research*, **17**, 63-72. https://doi.org/10.1016/0301-9268(82)90154-1

[33] Rollinson, H. (2016) Archaean Crustal Evolution in West Africa: A New Synthesis of the Archaean Geology in Sierra Leone, Liberia, Guinea and Ivory Coast. *Precambrian Research*, **281**, 1-12. https://doi.org/10.1016/j.precamres.2016.05.005

[34] Kouamelan, A.N., Djro, S.C., Allialy, M.E., Paquette, J.-L. and Peucat, J.-J. (2015)

The Oldest Rock of Ivory Coast. *Journal of African Earth Sciences*, **103**, 65-70. https://doi.org/10.1016/j.jafrearsci.2014.12.004

[35] Camil, J. (1984) Pétrographie, chronologie des ensembles archéens et formations associées de la région de Man (Côte d'Ivoire). Implications pour l'histoire géologique du craton ouest-africain, Thèse de l'Université d'Abidjan, 306 p.

[36] Juner, N.R. (1940) Geology of the Gold Coast and Western Togoland. Gold Coast Geol. Surv. Bull., Accra, No. 11, 40 p.

[37] Kesse, G.O. (1985) Geotraverse of the Birimian Systems in Southern Ghana. UNESCO Newsletter Bulletin, No. 4, 7-10.

[38] Lebrun, E., Thébaud, N., Miller, J., Ulrich, S., Bourget, J. and Terblanche, O. (2016) Geochronology and Lithostratigraphy of the Siguiri District: Implications for Gold Mineralization in the Siguiri Basin (Guinea, West Africa). *Precambrian Research*, **274**, 712-717. https://doi.org/10.1016/j.precamres.2015.10.011

[39] Fabre, R., Matheis, G. and Utke, A.W. (1987) Caractérisation géochimique du magmatisme birimien dans le centre de la Côte d'Ivoire (Afrique de l'Ouest). Ses implications géodynamiques. *Current Research in African Earth Sciences*: *Extended Abstracts of the* 14*th Colloquium on African Geology*, Berlin, 18-22 August 1987, 21-24.

[40] Sylvester, P.J. and Attoh, K. (1992) Lithostratigraphy and Composition of 2.1 Ga Greenstone Belts of the West African Craton and Their Bearing on Crustal Evolution and the Archean-Proterozoic Boundary. *Journal of Geology*, **100**, 377-393. https://doi.org/10.1086/629593

[41] Taylor, P.N., Moorbath, S., Leube, A. and Hirdes, W. (1992) Early Proterozoic Crustal Evolution in the Birimian of Ghana: Constrains from Geochronology and Isotope Geochemistry. *Precambrian Research*, **56**, 97-111. https://doi.org/10.1016/0301-9268(92)90086-4

[42] Pouclet, A., Vidal, M., Delor, C., Simeon, Y. and Alric, G. (1996) Le volcanisme birimien du nord-est de la Côte d'Ivoire, mise en évidence de deux phases volcano-tectoniques distinctes dans l'évolution géodynamique du Paléoprotérozoique. *Bulletin de la Société Géologique de France*, **167**, 529-541.

[43] Pouclet, A., Doumbia, S. and Vidal, M. (2006) Geodynamic Setting of the Birimian Volcanism in Central Ivory Coast (Western Africa) and Its Place in the Palaeoproterozoic Evolution of the Man Shield. *Bulletin de la Société Géologique de France*, **2**, 105-111. https://doi.org/10.2113/gssgfbull.177.2.105

[44] Baratoux, L., Mételka, V., Naba, S., Jessel, M.W., Grégoire, M. and Ganne, J. (2011) Juvenile Paleoproterozoic Crust Evolution during the Eburnean Orogeny (~2.2-2.0 Ga), Western Burkina Faso. *Precambrian Research*, **191**, 18-45. https://doi.org/10.1016/j.precamres.2011.08.010

[45] Bassot, J.-P. (1987) Le complexe volcano-plutonique calco-alcalin de la rivière Daléma (Est Sénégal): Discussion de sa signification géodynamique dans le cadre de l'orogénie eburnéenne (Protérozoïque inférieur). *Journal of African Earth Sciences*, **6**, 505-519. https://doi.org/10.1016/0899-5362(87)90091-1

[46] Klöckner Industrie (1989) Etude géologique des fenêtres protérozoïques inférieures du secteur du projet (Kayes, Kéniéba). Rapp. Techn., DNGM, Bamako, No. 1372.

[47] Dia, A., Van Schmus, W.R. and Kröner, A. (1997) Isotopic Constrains on the Age and Formation of a Paleoproterozoic Volcanic Arc Complex in the Kedougou Inlier, Eastern Senegal, West Africa. *Journal of African Earth Sciences*, **24**, 197-213. https://doi.org/10.1016/S0899-5362(97)00038-9

[48] Ndiaye, P.M., Dia, A., Viallete, Y., Diallo, P.D., Gom, P.M., Sylla, M., Wade, S. and

Dioh, E. (1997) Données pétrographiques, géochimiques, géochronologiques nouvelles sur les granitoïdes du Paléoprotérozoique du Supergroupe de Dialé-Daléma (Sénégal oriental): Implications pétrogénétiques et géodynamiques. *Journal of African Earth Sciences*, **25**, 193-208. https://doi.org/10.1016/S0899-5362(97)00098-5

[49] Lebrun, E., Thébaud, N., Miller, J., Ulrich, S., Bourget, J. and McCuaig, C.T. (2017) Structural Controls on an Orogenic Gold System: The World-Class Siguiri Gold District, Siguiri Basin, Guinea, West Africa. *Economic Geology*, **112**, 73-98. https://doi.org/10.2113/econgeo.112.1.73

[50] Doumbia, S., Pouclet, A., Kouamellan, A., Peucat, J.J., Vidal, M. and Delor, C. (1998) Petrogenesis of Juvenile-Type Birimian (Paleoproterozoic) Granitoids in Central Côte d'Ivoire, West Africa: Geochemistry and Geochronology. *Precambrian Research*, **87**, 33-63. https://doi.org/10.1016/S0301-9268(97)00201-5

[51] Gasquet, D., Barbey, P., Adou, P. and Paquette, J.L. (2003) Structure, Sr-Nd Isotope Geochemistry and Zircon U-Pb Geochronology of the Granitoids of the Dabakala Area (Côte d'Ivoire): Evidence for a 2.3 Ga Crustal Growth Event in the Paleoproterozoic of West Africa? *Precambrian Research*, **127**, 329-354. https://doi.org/10.1016/S0301-9268(03)00209-2

[52] Hirdes, W. and Davis, D.W. (1998) First U-Pb Zircon Age of Extrusive Volcanism in the Birimian Supergroup of Ghana/West Africa. *Journal of African Earth Sciences*, **27**, 291-294. https://doi.org/10.1016/S0899-5362(98)00062-1

[53] Davis, D.W., Hirdes, W., Schaltegger, U. and Nunoo, E.A. (1994) U-Pb Age Constraints on Deposition and Provenance of Birimian and Gold-Bearing Tarkwaian Sediments in Ghana, West Africa. *Precambrian Research*, **67**, 89-107. https://doi.org/10.1016/0301-9268(94)90006-X

[54] Ledru, P., Pons, J., Milesi, J.P., Feybesse, J.L. and Johan, V. (1991) Transcurrent Tectonics and Polycyclic Evolution in the Lower Proterozoic of Senegal-Mali. *Precambrian Research*, **50**, 337-354. https://doi.org/10.1016/0301-9268(91)90028-9

[55] Feybesse, J.-L. and Milési, J.-P. (1994) The Archaean/Proterozoic Contact Zone in West Africa: A Mountain Belt of Decollement Thrusting and Folding on a Continental Margin Related to 2.1 Ga Convergence of Archaean Cratons? *Precambrian Research*, **69**, 199-227. https://doi.org/10.1016/0301-9268(94)90087-6

[56] Caby, R., Delor, C. and Agoh, O. (2000) Lithologie, structure et métamorphisme des formations birimiennes dans la région d'Odienné (Côte d'Ivoire): Rôle majeur du diapirisme des plutons et des décrochements en bordure du craton de Man. *Journal of African Earth Sciences*, **30**, 351-374. https://doi.org/10.1016/S0899-5362(00)00024-5

[57] Bonhomme, M. (1962) Contribution à l'étude géochronologique de la plateforme de l'ouest-africain. Ann. Fac. Sci. Univ. Clermont-Ferrand, No. 5, 62 p.

[58] Milési, J.P., Feybesse, J.L., Ledru, P., Dommanget, A., Ouedraogo, M.F., Marcoux, E., Prost, A.E., Vinchon, C., Sylvain, J.P., Johan, V., Tegyey, M., Calvez, J.Y. and Lagny, P. (1989) Les minéralisations aurifères de l'Afrique de l'Ouest. Leurs rélations avec l'évolution lithostructurale au Protérozoïque inférieur. Chronique Recherche Minière, No. 497, 3-98.

[59] Vidal, M., Delor, C., Pouclet, A., Simeon, Y. and Alric, G. (1996) Evolution géodynamique de l'Afrique de l'Ouest entre 2,2 Ga et 2 Ga; le style archéen des ceintures vertes et des ensembles sédimentaires birimiens du nord-est de la Côte d'Ivoire. *Bulletin de la Société Géologique de France*, **167**, 307-319.

[60] Pons, J., Barbey, P., Dupuis, D. and Léger, J.M. (1995) Mechanisms of Pluton Emplacement and Structural Evolution of a 2.1 Ga Juvenile Continental Crust: The Bi-

rimian of Southwestern Niger. *Precambrian Research*, **70**, 281-301. https://doi.org/10.1016/0301-9268(94)00048-V

[61] Billa, M., Feybesse, J.-L., Bronner, G., Lerouge, C., Milési, J.-P., Traoré, S. and Diaby, S. (1999) Les formations à quartzite rubanés ferrugineux des monts Nimba et Simandou: Des unités empilées tectoniquement, sur un soubassement plutonique archéen (Craton de Kéneman-Man), lors de l'orogénèse Eburnéen. *Earth & Planetary Sciences*, **329**, 287-294. https://doi.org/10.1016/S1251-8050(99)80248-1

[62] Wane, O. (2010) Etude géologique du Birimien de la région de Massigui (paléoprotérozoïque du Mali méridional): La zone de cisaillement du Banifing, structure majeure du craton ouest-africain. Thèse de l'Université de Lille 1, 226 p.

[63] Black, R. (1980) Precambrian of West Africa. *Episodes*, **3**, 3-8. https://doi.org/10.18814/epiiugs/1980/v3i4/001

[64] Girard, P., Goulet, N. and Malo, M. (1998) Synthèse des données géologiques et cartographie. Amélioration et modernisation du centre de documentation. Géologie du Mali. Rapport final partie II. Projet d'assistance technique au secteur minier du Mali crédit 2390-M11.

[65] McFarlane, C.R.M., Mavrogenes, J., Lentz, D., King, K., Allibone, A. and Holcombe, R. (2011) Geology and Intrusion-Related Affinity of the Morila Gold Mine, Southeast Mali. *Economy Geology*, **106**, 727-750. https://doi.org/10.2113/econgeo.106.5.727

[66] Thiéblemont, D., Liégeois, J.P., Fernandez-Alonso, M., Ouabadi, A., Le Gall, B., Maury, R., Jalludin, M., Vidal, M., Ouattara Gbélé, C., Tchaméni, R., Michard, A., Nehlig, P., Rossi, P. and Chêne, F. (2016) Geological Map of Africa at 1:10 M Scale, CGMW-BRGM.

[67] Feybesse, J.-L., Sidibé, Y.T., Konaté, C.M., Lacomme, A., Zammit, C., Guerrot, C., Liégeois, J.-P., De Waelle, B., BRGM, CPG and DNGM (2006) Carte géologique de la République du Mali à 1/200000, Feuille n°NC-29-XVII, Tienko, Bamako (Mali): Ministère des mines, de l'Energie et de l'Eau, 2006.

[68] Feybesse, J.-L., Sidibé, Y.T., Konaté, C.M., Lacomme, A., Zammit, C., Guerrot, C., Liégeois, J.-P., De Waelle, B., BRGM, CPG and DNGM (2006) Notice explicative de la carte géologique de la République du Mali à 1/200000, Feuille n°NC-29-XVII, Tienko, Bamako (Mali): Ministère des mines, de l'Energie et de l'Eau, 2006. 32 p.

[69] Sangaré, A., Driouch, Y., Salvi, S., Femenias, O., Siebenaller, L., Belkasmi, M., Béziat, D., Dahire, M., Ntarmouchant, A., Adil, S. and Debat, P. (2014) Géologie des minéralisations aurifères du gisement tardi-éburnéen de Kalana (Birimien, Sud-Ouest du Mali). Bulletin de l'Institut Scientifique, Rabat, Sections Sciences de la Terre n°36, 85-108.

[70] Wassoul'or (2017) Optimisation des ressources du gisement d'or de Kodiéran. Unpublished Report, 280 p.

[71] Dao, O. (2019) Etude lithologique et métallogénique de la Mine d'Or de Faboula (Fenetre de Yanfolila, Mali sud). Mémoire de Master, Faculté des Sciences et Techniques (FST) de Bamako, 62 p.

[72] Ver Straeten, C.A. (2004) K-Bentonites, Volcanic Ash Preservation, and Implications for Early to Middle Devonian Volcanism in the Acadian Orogen, Eastern North America. *Bulletin of the Geological Society of America*, **116**, 474-489. https://doi.org/10.1130/B25244.1

[73] Salvi, S., Sangaré, A., Driouch, Y., Siebenaller, L., Béziat, D., Débat, P. and Femenias, O. (2016) The Kalana Vein-Hosted Gold Deposit, Southern Mali. *Ore Geology Reviews*, **78**, 599-605. https://doi.org/10.1016/j.oregeorev.2015.10.011

[74] Wane, O. (2019) The Eburnean Collision with the Kenema Man Craton: Evidences from the Paleoproterozoic Formations of the Massigui Degree Sheet (Southern Mali, Man Shield, West African Craton), Goldschmidt2019, Abstr. 3559.

[75] Wane, O., Femenias, O. and Lamouroux, C. (2007) Nature and Signification of Earlier Eburnean Structures Preserved inside the West African Craton Highlighted by a Detailed Structural Study of Banifing (Massigui Area, Southern Mali). Abstract, 5ème Coll. Int. 3MA: Magmatisme, Métamorphisme et Minéralisations associées. Fès, Maroc.

[76] Kusters, D. (2009) Multi-Stage Emplacement of Gold-Bearing Quartz Veins from Kalana Gold Mine Inferred by a Structural Survey. Master Sc. Geo., F.S. of ULB, 93 p.

[77] Miller, J.M., Davis, J., Baratoux, L., McCuaig, T.C., Metelka, V. and Jessel, M. (2013) Evolution of Gold Systems in Guinea, Southern Mali and Western Burkina Faso: AMIRA International Ltd P934A-West African Exploration Initiative-Stage 2 Final Unpublished Report, Appendix D1.

[78] Beattie, A.D., Hastings, P.E. and Storey, M.J. (1991) Kalana Mine, Rep. Unpublished. ZIMTECH, 62 p.

[79] Steyn, J.G. (2012) Structural Geology and Controls of Gold Mineralization in the Siguiri Mine, Guinea, West Africa. Thesis Degree Master of Science in Geology, Univ. Stellenbosch, 147 p.

[80] DiPietro, J.A. (2018) Chapter 20 California Strike-Slip System. In: DiPietro, J.A., Ed., *Geology and Landscape Evolution*, Second Edition, Elsevier, Amsterdam, 501-548. https://doi.org/10.1016/B978-0-12-811191-8.00020-8

[81] Fossen, H. (2010) Structural Geology. Cambridge University Press, Cambridge, 481 p.

[82] Ouologuem, A.B. (2019) Etude pétrographique et structurale des lithologies paléoprotérozoïques de la Mine d'Or de Faboula (Fenêtre de Yanfolila, Mali, Mali sud). Mem. Master. FST-USTTB, 76 p.